

Kaluza–Klein excitations of gauge bosons at the LHC

Abdelhak Djouadi¹, Grégory Moreau¹, Ritesh K. Singh^{1,2}

¹ Laboratoire de Physique Théorique, CNRS and Université Paris–Sud,
Bât. 210, F–91405 Orsay Cedex, France.

² Laboratoire de Physique Théorique, LAPTH, F–74941 Annecy–le–Vieux, France.

Abstract

We consider the Randall–Sundrum extra dimensional model with fields propagating in the bulk based on an extended electroweak gauge symmetry with specific fermion charges and localizations that allow to explain the LEP anomaly of the forward–backward asymmetry for b -quarks, A_{FB}^b . We study the manifestations of the strongly–interacting and electroweak gauge boson Kaluza–Klein excitations V_{KK} at the LHC, with masses of the order of a few TeV, which dominantly decays into top and bottom quark pairs. We first analyze the two–body tree–level production processes $pp \rightarrow t\bar{t}$ and $b\bar{b}$ in which the Kaluza–Klein (KK) excitations of gauge bosons are exchanged. We find that the additional channels can lead to a significant excess of events with respect to the Standard Model prediction; characteristic top quark polarization and angular asymmetries are quantitatively studied and turn out to probe the chiral structure of couplings to excited states. We then analyze higher order production processes for the gauge boson excitations which have too weak or no couplings to light quarks and, in particular, the loop induced process $gg \rightarrow V_{KK} \rightarrow t\bar{t}$ and $b\bar{b}$ in which the anomalous ggV_{KK} four–dimensional vertex has to be regulated. The RS effects in this process, as well as in the four–body reactions $pp \rightarrow t\bar{t}b\bar{b}$, $t\bar{t}t\bar{t}$, $b\bar{b}b\bar{b}$ and in the related three–body reactions $gb \rightarrow bt\bar{t}$, $bb\bar{b}$, in which the V_{KK} excitations are mainly radiated off the heavy quarks, are shown to be potentially difficult to test at LHC, due to small phase space and low parton density for $M_{KK} \gtrsim 3$ TeV.

1. Introduction

Among the extra-dimensional models which have been proposed in the recent years as extensions of the Standard Model (SM), the one of Randall and Sundrum (RS) [1] seems to be particularly attractive. First, it addresses the gauge hierarchy problem without introducing a new energy scale in the fundamental theory. Moreover, the variant in which the SM fermions and gauge bosons are propagating in the bulk allows for the unification of the gauge coupling constants at high energies [2] and provides a viable candidate of Kaluza–Klein (KK) type for the Dark Matter of the universe [3]. This version of the RS model with bulk matter offers also the possibility, through a simple geometrical mechanism, of generating the large mass hierarchies prevailing among SM fermions [4–6]. Indeed, if the various fermions are placed along the extra dimension, their different wave functions overlap with the Higgs boson, which remains confined on the so-called TeV-brane for its mass to be protected, generate hierarchical patterns among the effective four-dimensional Yukawa couplings.

If this extra-dimensional model is to solve the gauge hierarchy problem, the masses of the first KK excitations of the SM gauge bosons, M_{KK} , must be in the vicinity of the TeV scale. The direct experimental search for KK gluon excitations at Tevatron Run II leads to the bound $M_{\text{KK}} \gtrsim 800$ GeV [7]. The high-precision measurements impose strong lower bounds on M_{KK} as the exchanges of the KK excitations lead to new and unacceptably large contributions to the electroweak observables [8]. Nevertheless, it was shown [9] that if the SM gauge symmetry is enhanced to the left–right structure $\text{SU}(2)_L \times \text{SU}(2)_R \times \text{U}(1)_{B-L}$, with B and L being respectively the baryon and lepton numbers, the high-precision data can be nicely fitted while keeping the masses down to an acceptable value¹ of $M_{\text{KK}} \simeq 3$ TeV, this lower limit being quite independent of the geometry of the extra dimension [11].

Instead of the $\text{U}(1)_{B-L}$ group in the extended gauge symmetry as originally proposed in Ref. [9], other $\text{U}(1)_X$ groups with different fermion charges can be considered [12, 13]. An important motivation is that with specific charges of the new Abelian group and for specific fermion localizations, different from the ones considered in Ref. [9], the three standard discrepancy between the forward–backward asymmetry A_{FB}^b in Z decays to bottom quarks measured at LEP and elsewhere [14, 15] and the SM prediction [16] is naturally resolved, while keeping all the other electroweak precision observables, including the partial decay width of the Z boson into b -quarks $R_b \equiv \Gamma(Z \rightarrow b\bar{b})/\Gamma(Z \rightarrow \text{hadrons})$, unaffected and in agreement with the data. More precisely, in the framework presented in Refs. [12, 13], the measured values of the asymmetry $A_{FB}^b(\sqrt{s})$ can be reproduced both at LEP1 [14], i.e. on the Z pole, and at energies outside the Z -pole [15], while with the charge assignments of $\text{U}(1)_{B-L}$, the measured value of the asymmetry cannot be reproduced at energies lower than LEP1; see Ref. [13] for a detailed discussion.

¹The severe indirect bounds on M_{KK} from precision data could also be softened down to a few TeV in scenarios with brane-localized kinetic terms for fermions and gauge bosons [10].

The resolution of the A_{FB}^b LEP anomaly is essentially due to the fact that since the third generation fermions should be localized closer to the TeV-brane to get higher masses, their couplings to the KK gauge bosons, which are typically located near the TeV-brane, are larger and generate more important contributions to electroweak observables in the b sector. One needs also to take into account the tension between generating a large mass to the top quark, which requires the left-handed doublet $(t, b)_L$ to be near the TeV-brane, and satisfying the bounds from precision data that constrain the $Zb_L\bar{b}_L$ coupling to be almost SM-like, which forces the $(t, b)_L$ doublet [via the mixing of the Z boson with the KK states] to have small couplings to the KK gauge bosons and thus to be far from the TeV-brane. However, for a suitable choice of the $(t, b)_L$ representation under $SU(2)_R$, the KK corrections to the coupling $Zb_L\bar{b}_L$ can be suppressed [12, 17]. Alternatively, the tension is softened in the framework of Ref. [13] summarized above, in which the $Zb_L\bar{b}_L$ and $Zb_R\bar{b}_R$ couplings are chosen so that the electroweak precision data are reproduced².

Thus and, generically speaking, in the context of the RS model with SM fields in the bulk, the KK gauge bosons dominantly couple to heavy SM fermions as they are localized toward the TeV-brane (this typical feature can only be avoided in some particular situations [21]). In this case, the processes involving the third generation b and t quarks are those which are expected to be significantly affected by the presence of the new vector states. In Ref. [13, 22], the impact of the KK excitations of the electroweak gauge bosons has been discussed in the context of heavy flavor production at high energy e^+e^- colliders (ILC). Because of the high precision which can be achieved in the measurement of the production rates and polarization/angular asymmetries in the $e^+e^- \rightarrow t\bar{t}, b\bar{b}$ processes at the ILC, KK vector excitations with large masses can be probed, provided that they have non-vanishing couplings also to the initial light leptons. However, because of the limited energy of the ILC, $\sqrt{s} = 0.5\text{--}1$ TeV, and the expected large V_{KK} masses, $M_{KK} \sim$ a few TeV, the particles are accessible only indirectly through their virtual exchange.

At the Large Hadron Collider (LHC), the energy is principle sufficient to produce directly the KK excitations of the gluons and the electroweak gauge bosons with masses in the multi-TeV range. The most direct manifestation of these KK states³ would be their production in the Drell-Yan processes, $pp \rightarrow V_{KK} = g^{(1)}, \gamma^{(1)}, Z^{(1)}, Z'^{(1)}$. However, in contrast to the (standard) production at the LHC of extra Z' bosons from Grand Unified Theories (GUTs) [25] and to some universal extra-dimensional models [26]⁴, there are many difficulties in the

²Note that there are also constraints on the top and bottom quark couplings from Flavour Changing Neutral Current (FCNC) processes, but those can be satisfied for M_{KK} values around the TeV scale Ref. [18–20].

³Another possibility to probe this variant of the RS scenario at LHC is to look for the production of KK gravitons [23], or, the new quarks that are present in the model [24]. In the present analysis, we do not discuss these possibilities and we assume that the new fermionic states are too heavy and do not end up as decay products of the KK gauge bosons.

⁴In Ref. [26], this mechanism has been studied at the LHC in RS models with bulk matter but with

present scenario. The first one is that, contrary to the new Z 's of GUTs, the KK excitations present in this model have rather tiny couplings to the light fermions and large couplings to the heavy quarks. On the one hand, the production cross sections in the Drell–Yan process $q\bar{q} \rightarrow V_{\text{KK}}$ are much smaller, the probability of finding a heavy quark in the proton being tiny; in fact, in the case of the excitations of the extra Z' , which is a superposition of the Z_R and Z_X bosons of the extended $\text{SU}(2)_R \times \text{U}(1)_X$ group, the couplings to light fermions are almost negligible and Drell–Yan production does not occur [except through $b\bar{b} \rightarrow Z'^{(1)}$ which gives a small contribution due to the reduced b -quark density in the proton]. On the other hand, because of their large couplings to heavy fermions, the new KK excitations will decay almost exclusively into $t\bar{t}$ and $b\bar{b}$ final states; these topologies have a less striking signature than the GUTS $Z' \rightarrow \ell^+\ell$ with $\ell = e, \mu$ channel and are subject to a much more severe background at the LHC. Another difficulty, that is related to the previous one, lies in the fact that because of the strong couplings to heavy fermions, the KK excitations have large total decay widths and are not anymore narrow resonances. This will complicate the searches for these states since in the processes $p\bar{p} \rightarrow V_{\text{KK}} \rightarrow t\bar{t}$ or $b\bar{b}$, the corresponding QCD backgrounds become also large as they have to be integrated in wider bins [28, 29].

There are two other possibilities of observing the heavy KK states. The first one is single V_{KK} production in the gluon–gluon fusion mechanism $gg \rightarrow V_{\text{KK}}$ which is mediated by heavy $Q = t, b$ quark loops⁵; because of the chirality dependence of $V_{\text{KK}}t\bar{t}$ and $V_{\text{KK}}b\bar{b}$ four-dimensional effective couplings, the one-loop effective ggV_{KK} vertex is anomalous and the chiral anomaly has to be regulated by considering the Stückelberg mixing term (for a review on the topic, see e.g. Ref. [30]). The second possibility is associated production with heavy quark pairs, $pp \rightarrow gg/q\bar{q} \rightarrow Q\bar{Q}V_{\text{KK}}$ with $Q = t, b$, leading to $b\bar{b}t\bar{t}, b\bar{b}b\bar{b}$ and $t\bar{t}t\bar{t}$ final states; another mechanism, which is related to the later class of processes would be the two-body process $gb \rightarrow bV_{\text{KK}} \rightarrow b\bar{b}, bt\bar{t}$ where the initial bottom parton is taken from the proton sea⁶. In fact, when the couplings of the KK states to light quarks are small and the Drell–Yan process is not effective, these mechanisms are the only possibilities which give access to the new states; this is the case for the production of the KK excitation of the new Z' boson for instance. However, because these processes are of higher order in perturbation theory, the production cross sections are not substantial despite the fact that the couplings which are involved are large. Nevertheless, in view of the interesting final state signature, a better control of the corresponding QCD backgrounds might be possible.

the hypothesis of a universal fermion profile [made in order to totally suppress FCNC effects] which are not compatible with an interpretation of fermion mass hierarchies through the wave function overlap mechanism.

⁵The process $gg \rightarrow V_{\text{KK}} \rightarrow t\bar{t}$ has been first suggested in Ref. [9] and recently mentioned in Ref. [27]; however, because of Yang's theorem the vector part of the ggV_{KK} coupling will give zero contribution while the axial part of the coupling will give a finite contribution only if the V_{KK} state is virtual and, thus, if its total width is included.

⁶ This second class of processes have also been discussed in Ref. [31] for rather general scalar and vector resonances which couple to top and bottom quarks with the same strength.

In the present paper, we perform a complete study of the Drell–Yan and gluon fusion processes $q\bar{q}, gg \rightarrow b\bar{b}, t\bar{t}$ as well as the associated production $q\bar{q}/gg \rightarrow b\bar{b}t\bar{t}, b\bar{b}b\bar{b}, t\bar{t}t\bar{t}$ and $gb \rightarrow b\bar{b}, b\bar{t}\bar{t}$ processes at the LHC, in the RS model with bulk matter. We will base our analysis on the framework which resolves the A_{FB}^b anomaly [13], but the results that we obtain can be easily generalized to other scenarios. In a parton–level analysis which includes only the dominant QCD backgrounds, we show that for a set of characteristic points of the parameter space, the exchange of KK gauge bosons [excitations of the gluon as well as of the electroweak bosons γ, Z and new Z'] can lead to visible deviations with respect to the SM production rates in the Drell–Yan process $pp \rightarrow V_{\text{KK}} \rightarrow b\bar{b}, t\bar{t}$. For the latter reaction, the signal rates are large and some top polarization and asymmetries allow to test the chiral couplings to the KK modes. In the case where the KK excitations have too small couplings to the light quarks, the loop induced gluon fusion mechanism $gg \rightarrow t\bar{t}$ and $b\bar{b}$ as well as the associated production mechanisms $pp \rightarrow Q\bar{Q}V_{\text{KK}} \rightarrow b\bar{b}t\bar{t}$ and $gb \rightarrow b\bar{t}\bar{t}$, with an excess in the top or bottom pair invariant mass distributions can be in principle exploited. However, because of the large mass of the KK excitations assumed in this study, the signal significance turns out to be small, except potentially, for the $gb \rightarrow b\bar{t}\bar{t}$ process.

Note that while the present analysis was on–going, the on–shell production of KK gluons decaying into top quarks, $pp \rightarrow g^{(1)} \rightarrow t\bar{t}$ has been studied at the LHC [27, 28] in the framework developed in Ref. [9] with the left–right extended gauge structure. The $pp \rightarrow b\bar{b}$ process has not been considered as it is expected to be less significant than in the framework [13] considered here where the right–handed b quark is closer to the TeV–brane, with an increased coupling to KK gauge bosons; also in this case, the cross section for $t\bar{t}$ production would be different as b coupling variations modify e.g. the KK gluon total width as well as the $b\bar{b}$ parton initial state contribution (especially as here b_R is closer to the TeV–brane so that it can get a non–vanishing coupling to the Z'). Note also that the production of the excitations of the electroweak gauge bosons as well as higher order processes (including 3 and 4 quark final states) have not been considered in Ref. [27, 28] (in [27] the emphasis was put on the determination of excitation spin and methods of highly energetic top identification).

The paper is organized as follows. In the next section, we briefly describe the theoretical framework in which we will work and the considered scenarios which will be used for illustration; the decays of the KK states will also be summarized. In section 3, the signal of the KK excitations at the LHC in the Drell–Yan processes $pp \rightarrow t\bar{t}, b\bar{b}$ and the corresponding irreducible QCD backgrounds are analyzed; relevant polarization and angular asymmetries are studied in details. In section 4, we discuss the gluon fusion mechanism $gg \rightarrow V_{\text{KK}} \rightarrow t\bar{t}, b\bar{b}$ and briefly the associated production processes with $t\bar{t}/b\bar{b}$ pairs and those with a b -quark, as well as their corresponding QCD backgrounds. A brief conclusion will be given in section 5.

2. Physical framework

2.1 The specific RS extension

In this paper, we consider the RS model in which SM fields propagate along the extra spatial dimension, like gravity, but the Higgs boson remains confined on the TeV-brane. In the RS scenario, the warped extra dimension is compactified over a S^1/\mathbb{Z}_2 orbifold. While the gravity scale on the Planck-brane is $M_P = 2.44 \times 10^{18}$ GeV, the effective scale on the TeV-brane, $M_\star = e^{-\pi k R_c} M_P$, is suppressed by a warp factor which depends on the curvature radius of the anti-de Sitter space $1/k$ and the compactification radius R_c . The product $kR_c \simeq 11$ leads to $M_\star = \mathcal{O}(1)$ TeV, thus addressing the gauge hierarchy problem.

The fermion mass values are dictated by their wave function localization. In order to control these localizations, the five-dimensional fermion fields Ψ_i , with $i = 1, 2, 3$ being the generation index, are usually coupled to distinct masses m_i in the fundamental theory. If $m_i = \text{sign}(y)c_i k$, where y parameterizes the fifth dimension and c_i are dimensionless parameters, the fields decompose as $\Psi_i(x^\mu, y) = \sum_{n=0}^{\infty} \psi_i^{(n)}(x^\mu) f_n^i(y)$, where n labels the tower of KK excitations and $f_0^i(y) = e^{(2-c_i)k|y|}/N_0^i$ with N_0^i being a normalization factor. Hence, as c_i increases, the wave function $f_0^i(y)$ tends to approach the Planck-brane at $y = 0$.

In order to protect the electroweak observables against large deviations and, at the same time, to resolve the anomaly in the forward-backward asymmetry for b -quark production A_{FB}^b , the electroweak gauge symmetry is enhanced to $SU(2)_L \times SU(2)_R \times U(1)_X$ with the following fermion representations/charges under the group gauge [12, 13]:

$$\begin{aligned}
 Q_L^i &\equiv (\mathbf{2}, \mathbf{1})_{\frac{1}{6}}; & u_R^i &\in (\mathbf{1}, \mathbf{2})_{\frac{1}{6}} \text{ with } I_{3R}^{u_R^i} = +\frac{1}{2}; \\
 & & d_R^i &\in (\mathbf{1}, \mathbf{2})_{-\frac{5}{6}} \text{ with } I_{3R}^{d_R^i} = +\frac{1}{2} \\
 L_L^i &\equiv (\mathbf{2}, \mathbf{1})_{-\frac{1}{2}}; & \ell_R^i &\in (\mathbf{1}, \mathbf{2})_{-\frac{1}{2}} \text{ with } I_{3R}^{\ell_R^i} = -\frac{1}{2}
 \end{aligned} \tag{1}$$

respectively for the left-handed $SU(2)_L$ doublets of quarks, right-handed up/down type quarks, doublets of leptons and right-handed charged leptons. The usual symmetry of the SM is recovered after the breaking of both $SU(2)_R$ and $U(1)_X$ on the Planck-brane, with possibly a small breaking of the $SU(2)_R$ group in the bulk. Note the appearance of a new Z' boson [but without a zero-mode] which is a superposition of the state \widetilde{W}^3 associated to the $SU(2)_R$ group and \widetilde{B} associated to the $U(1)_X$ factor; the orthogonal state is the SM hypercharge B boson. Up-type quarks acquire masses through a Yukawa interaction of type $\overline{(\mathbf{2}, \mathbf{1})_{\frac{1}{6}}}(\mathbf{2}, \mathbf{2})_0(\mathbf{1}, \mathbf{2})_{\frac{1}{6}}$, the Higgs boson being embedded in a bidoublet of $SU(2)_L \times SU(2)_R$. Because of their specific $SU(2)_R$ isospin assignment $I_{3R}^{d_R^i}$, down-type quarks become massive via another kind of invariant operator as in Ref. [12, 13].

2.2 EW constraints and the fermion couplings

From the theoretical point of view, solving the gauge hierarchy problem forces the masses of the first KK excitations of the SM gauge bosons, $M_{\text{KK}} = M_{\gamma^{(1)}} = M_{g^{(1)}} \simeq M_{Z^{(1)}} \simeq M_{Z'^{(1)}}$, to be of order the TeV scale. Indeed, one has $M_{\text{KK}} = 2.45kM_\star/M_P \lesssim M_\star = \mathcal{O}(\text{TeV})$ since the theoretical consistency bound on the five-dimensional curvature scalar leads to $k < 0.105M_P$. More precisely, the maximal value of M_{KK} is fixed by this theoretical consistency bound and the kR_c value. One could consider a maximal value of $M_{\text{KK}} \simeq 10$ TeV which corresponds to $kR_c = 10.11$. From the experimental point of view, as mentioned previously, the electroweak (EW) high-precision data force the KK mass to be larger than $M_{\text{KK}} \sim 3$ TeV. Given these theoretical and experimental considerations, we will fix the masses of the KK excitations to a common value $M_{\text{KK}} = 3$ TeV in the present study.

With light SM fermions [leptons and first/second generation quarks] characterized by $c_{\text{light}} > 0.5$, c being the parameter which determines the fermion localization as discussed in the subsection above, the bulk custodial isospin gauge symmetry insures an acceptable fit of the oblique corrections to electroweak observables for $M_{\text{KK}} \gtrsim 3$ TeV [9]. The large value of the top quark mass requires $c_{t_R} < 0.5$ and $c_{Q_L^3} < 0.5$, with $c_{Q_L^3} = c_{t_L} = c_{b_L}$ [as the states b_L and t_L belong to the same $\text{SU}(2)_L$ multiplet] so that the top and bottom quarks have to be treated separately in the studies of the electroweak precision data. In the framework developed in Ref. [13], the precision data in the b sector, that is, the b -quark forward-backward asymmetry A_{FB}^b and the $b\bar{b}$ partial decay width of the Z boson $R_b \equiv \Gamma(Z \rightarrow b\bar{b})/\Gamma(Z \rightarrow \text{hadrons})$, are correctly reproduced with $M_{\text{KK}} = 3$ TeV for certain values of the c parameters depending on the coupling constant $g_{Z'}$ of the new Z' boson.

For instance, if the coupling $g_{Z'}$ is equal to $0.6\sqrt{4\pi}$, the best fit of the observables R_b measured at LEP1 and $A_{FB}^b(\sqrt{s})$ measured at various center-of-mass energies is obtained for $c_{Q_L^3} \simeq 0.36$ and $c_{b_R} \simeq 0.438$ [the fit corresponds to $\chi_{\text{RS}}^2 \simeq 14$ and substantially improves the one in the SM, $\chi_{\text{SM}}^2 \simeq 24$]. For this c_{b_R} value, one obtains the values $Q(c_{b_R}) \simeq 0.55$ and $Q'(c_{b_R}) \simeq 0.75$, where $Q(c)$ ($Q'(c)$) is the ratio of the four-dimensional effective coupling between the $g^{(1)}/\gamma^{(1)}/Z^{(1)}$ ($Z'^{(1)}$) boson and the SM fermions, over the coupling of the gluon/photon/ Z (would be Z') boson zero-mode. In fact, the value chosen above for the $g_{Z'}$ coupling is close to the typical limit obtained from the perturbativity condition, $2\pi kR_c g_{Z'}^2/16\pi^2 < 1$, for the coupling of the KK excitation of the Z' boson, when quantum corrections are included. Indeed, the effective four-dimensional coupling of the $Z'^{(1)}$ boson to SM fields is increased by a factor as large as $\sqrt{2\pi kR_c}$ relatively to $g_{Z'}$ for SM fields near the TeV-brane, like for example the Higgs boson⁷.

For the choice $g_{Z'} = 0.3\sqrt{4\pi}$, the best fit of R_b and $A_{FB}^b(\sqrt{s})$ [still corresponding to a

⁷A bound of the same order can be derived from considerations on the strong coupling regime of the five-dimensional theory: perturbativity imposes that the five-dimensional loop expansion parameter, estimated at an energy k to be $\sim (g_{Z'}^{5D})^2 k/16\pi^2 = \pi kR_c g_{Z'}^2/16\pi^2$, should be smaller than unity [32].

good fit of the data, $\chi^2 \simeq 14$] is obtained for the c values $c_{Q_L^3} \simeq 0.36$ and $c_{b_R} \simeq 0.135$, leading to the charges $Q(c_{b_R}) \simeq 3.0$ and $Q'(c_{b_R}) \simeq 3.2$. For this value of $c_{Q_L^3}$, one obtains for instance a top quark mass $m_t \simeq 90$ GeV or $m_t \simeq 80$ GeV with, respectively, $c_{t_R} \simeq -0.3$ or $c_{t_R} \simeq +0.1$, which are in the correct order of magnitude. In order to determine the set of parameters that would reproduce exactly the measured m_t value, one need to study the full three-flavour mass matrix [by fixing also each Yukawa coupling constant] and include the effect of mixing between t and its KK excitations, which is beyond the scope of this work. For $c_{Q_L^3} \simeq 0.36$ and $c_{b_R} \simeq 0.438$, the bottom mass has also a correct order of magnitude. The bottom and top quark Yukawa couplings have different gauge structures in the present context and the bottom Yukawa coupling constant could be taken smaller (while choosing a smaller c_{b_R} , in order to still generate a satisfactory bottom mass) as proposed in Ref. [12] in order to have a weak breaking of the custodial symmetry subgroup protecting the $Zb_L\bar{b}_L$ coupling.

In this study, we will consider four typical scenarios which are defined by the c assignments for the top and bottom quarks and the value of the coupling $g_{Z'}$; these parameters and their corresponding $Q(c)$ and $Q'(c)$ charges are summarized in Table 1. In the four points of parameter space, labeled $E_{1,2,3,4}$, the assignment for the left-handed (t, b) doublet, $c_{Q_L^3} = 0.36$ which leads to the charges $Q(c_{Q_L^3}) = 1.34$ and $Q'(c_{Q_L^3}) = 1.52$, has been adopted in order to reproduce the experimental values of A_{FB}^b and R_b . For the light fermions, i.e. the leptons and the first and second generation quarks, we will set $c_{\text{light}} \gtrsim 0.5$, as necessary to generate sufficiently small masses. This leads to a small Q charge for these fermions, $Q(c_{\text{light}}) \simeq -0.2$, and a zero Z' charge, $Q'(c_{\text{light}}) = 0$. This means that the couplings of the KK excitations of the gluon, photon and Z boson have small couplings to light fermions compared to the top and bottom quarks [an order of magnitude smaller in general], while the KK excitations of the Z' boson do not couple to these light fermions at all.

	$g_{Z'}$	c_{b_R}	$Q(c_{b_R})$	$Q'(c_{b_R})$	c_{t_R}	$Q(c_{t_R})$	$Q'(c_{t_R})$
E_1	$0.6\sqrt{4\pi}$	0.438	0.55	0.75	-0.3	4.90	5.01
E_2	$0.3\sqrt{4\pi}$	0.135	3.04	3.19	-0.3	4.90	5.01
E_3	$0.6\sqrt{4\pi}$	0.438	0.55	0.75	+0.1	3.25	3.40
E_4	$0.3\sqrt{4\pi}$	0.135	3.04	3.19	+0.1	3.25	3.40

Table 1: The four scenarios labeled $E_{1,\dots,4}$ to be considered in this study and their respective c assignments, $Q(c)$, $Q'(c)$ charges and $g_{Z'}$ couplings. The other (common) parameters are $c_{Q_L^3} = 0.36$, which leads to $Q(c_{Q_L^3}) = 1.34$ and $Q'(c_{Q_L^3}) = 1.52$, and $c_{\text{light}} \gtrsim 0.5$, for which $Q(c_{\text{light}}) = -0.2$ and $Q'(c_{\text{light}}) = 0$; $M_{\text{KK}} = 3$ TeV.

2.3 Decays of the KK gauge bosons

The KK excitations of the gauge bosons will decay into pairs of SM fermions, $V_{\text{KK}} \rightarrow f\bar{f}$; as mentioned previously, we will assume that all the KK excitations of the fermions, as well as the zero-modes of the new fermions that are present in the model, are too heavy, $2m_f \gtrsim M_{V_{\text{KK}}}$, so that they do not appear in the decays of the KK gauge bosons. The partial decay width of V_{KK} into a fermion species f is given by

$$\Gamma(V_{\text{KK}} \rightarrow f\bar{f}) = \frac{M_{V_{\text{KK}}}\beta_f C_f^{V_{\text{KK}}}}{24\pi} \left[\frac{3 + \beta_f^2}{4} ((g_{f_L}^{V_{\text{KK}}})^2 + (g_{f_R}^{V_{\text{KK}}})^2) + \frac{3(\beta_f^2 - 1)}{2} g_{f_L}^{V_{\text{KK}}} g_{f_R}^{V_{\text{KK}}} \right] \quad (2)$$

where m_f is the mass of the fermion f , $\beta_f = \sqrt{1 - 4m_f^2/M_{V_{\text{KK}}}^2}$ its velocity in the rest frame of the KK gauge boson and $C_f^{V_{\text{KK}}}$ the color factor: $C_q^{V_{\text{KK}}} = 3$, $C_\ell^{V_{\text{KK}}} = 1$ for electroweak boson couplings to, respectively, quarks and leptons and $C_q^{g^{(1)}} = \frac{1}{2}$, $C_\ell^{g^{(1)}} = 0$ for the coupling of the KK gluon to quarks and colorless fermions. The left- and right-handed couplings of the KK gauge boson V_{KK} to the fermion f are denoted by $g_{f_L}^{V_{\text{KK}}}$ and $g_{f_R}^{V_{\text{KK}}}$; in terms of the couplings of the corresponding zero-mode, $g_{f_{L/R}}^V$, they are given by $g_{f_{L/R}}^{V_{\text{KK}}} = g_{f_{L/R}}^V Q^{(\prime)}(c_{f_{L/R}})$, with $Q(c_{f_{L/R}})$ and $Q'(c_{f_{L/R}})$ as defined in the previous subsection and given in Table 1. The total decay width of the KK excitation is simply $\Gamma_{V_{\text{KK}}} = \sum_f \Gamma(V_{\text{KK}} \rightarrow f\bar{f})$, where the sum runs over all SM fermions.

Because the KK gauge boson couplings to fermions are directly proportional to the charges $Q(c)$ and $Q'(c)$, the partial decay widths $\Gamma(V_{\text{KK}} \rightarrow f\bar{f}) \propto (g_{f_L}^{V_{\text{KK}}})^2 + (g_{f_R}^{V_{\text{KK}}})^2$ in the limit $M_{V_{\text{KK}}} \gg m_f$, are typically two orders of magnitude larger in the case of final state top and bottom quarks than for the light fermions. The branching ratios $\text{BR}(V_{\text{KK}} \rightarrow t\bar{t})$ and $\text{BR}(V_{\text{KK}} \rightarrow b\bar{b})$, with $V_{\text{KK}} = \gamma^{(1)}$, $Z^{(1)}$, $Z'^{(1)}$ and $g^{(1)}$, are displayed in Table 2 in the four scenarios $E_{1,\dots,4}$ introduced previously. As can be seen, the sum of these two branching ratios is close to unity which means that the KK excitations decay almost exclusively into the heavy t, b quarks and that little room is left for decays into light quarks and leptons [in fact, there is no room at all for these decays in the case of the $Z'^{(1)}$ boson as the charge $Q'(c_{\text{light}})$ is zero]. In our analysis, we will therefore concentrate on the t, b final state decay products of the KK gauge bosons.

Finally, the total decay widths of the KK excitations V_{KK} are also given in Table 2 for the four scenarios. As they grow proportionally to the mass $M_{V_{\text{KK}}}$, they are rather large for the value $M_{\text{KK}} = 3$ TeV. For instance, the decay width of the KK gluon is of the order of a few hundred GeV and is between 10% and 20% of the $g^{(1)}$ mass; the KK state can be thus considered as a relatively narrow resonance. Due to the significant $g_{Z'}$ values taken, the total decay widths are smaller for the KK excitations of the photon and Z boson than for the KK excitation of the Z' boson. In the latter case, the total width is comparable to the $Z'^{(1)}$ mass and one can hardly consider the state as a true resonance.

	$g^{(1)}$	$\gamma^{(1)}$	$Z^{(1)}$	$Z'^{(1)}$
E_1	627/0.08/0.91	137/0.02/0.96	75/0.28/0.68	3360/0.02/0.98
E_2	828/0.30/0.69	149/0.10/0.89	79/0.31/0.65	1080/0.29/0.71
E_3	328/0.14/0.83	68.0/0.04/0.93	54/0.39/0.56	1580/0.04/0.96
E_4	530/0.47/0.52	80.0/0.18/0.79	58/0.43/0.53	661.0/0.47/0.53

Table 2: The total decay widths (in GeV) and the $b\bar{b}$ and $t\bar{t}$ branching ratios of the first KK excitations of the gluon, photon, Z and Z' bosons in the four selected scenarios E_1, \dots, E_4 for $M_{\text{KK}} = 3$ TeV: $\Gamma_{V_{\text{KK}}}/\text{BR}(V_{\text{KK}} \rightarrow b\bar{b})/\text{BR}(V_{\text{KK}} \rightarrow t\bar{t})$.

3. Top and bottom quark pair production

3.1 General features

The most straightforward way to produce the KK excitations of the gauge bosons⁸ V_{KK} at the LHC is via the Drell–Yan process,

$$pp \rightarrow q\bar{q} \rightarrow V_{\text{KK}} \rightarrow Q\bar{Q}, \quad Q = t, b \quad (3)$$

with the gauge bosons V_{KK} subsequently decaying into top and bottom quarks; Fig. 1a. As discussed previously, V_{KK} decays into the light fermion states [leptons and first/second generation quarks] will be neglected as their branching ratios are very small in the framework that we are considering here. The relatively small couplings of the initial quarks $q \equiv u, d, s, c$ to V_{KK} lead to smaller production rates compared to, for instance, the production of Z' bosons from GUTs which have full–strength couplings to light fermions. Because the V_{KK} couplings to bottom quarks are large, the partonic cross section from the subprocess $b\bar{b} \rightarrow V_{\text{KK}}$ would, in principle, be more substantial than for the $q\bar{q} \rightarrow V_{\text{KK}}$ subprocesses but, after folding with the smaller b -parton density, the corresponding hadronic cross section is reduced. Note that since the KK gauge bosons have different couplings to left- and right-handed fermions, one expects the produced t/b quarks to be polarized and to have a forward–backward asymmetry.

Because the KK excitations have substantial total decay widths [see Table 2], the narrow width approximation in which the production and decay processes are factorized and considered separately is not sufficient. Indeed, one needs to consider the virtual exchange of the KK excitations in which the total width is included in a Breit–Wigner form, together with the exchange of the zero modes. The full interference between the zero and first modes of the gluon, on the one hand, and of the electroweak bosons, on the other hand, should be taken into account [because of color conservation, there is no interference between the

⁸From now on, we will restrict ourselves to the first KK excitations, $V_{\text{KK}} = \gamma^{(1)}, Z^{(1)}, Z'^{(1)}$ and $g^{(1)}$.

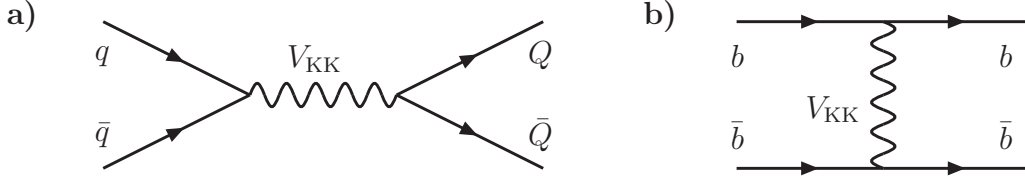


Figure 1: Feynman diagram for heavy $Q = t, b$ quark pair production at the LHC through $q\bar{q}$ annihilation, where q stands for initial state quarks and KK for the KK excitations of neutral gauge bosons, namely $\gamma^{(n)}$, $g^{(n)}$, $Z^{(n)}$ and $Z'^{(n)}$ with $n = 0, 1, 2, \dots$ being the KK level; mainly the zero-modes $n = 0$, except for Z' , and the first KK excitations $n = 1$ contribute to the signal. For bottom quark production there is an additional t -channel diagram exchanging neutral KK gauge bosons with bottom partons in the initial state (b).

amplitudes in which the gluon and the electroweak gauge bosons are exchanged]. For the $b\bar{b}$ production, the subprocesses are also initiated by bottom partons and one should also consider the channel in which the KK gauge bosons are exchanged in the t -channel; Fig. 1b.

The signal for the KK gauge bosons $q\bar{q} \rightarrow V_{KK} \rightarrow Q\bar{Q}$ and the main SM background $q\bar{q} \rightarrow Q\bar{Q}$ and $gg \rightarrow Q\bar{Q}$ have to be considered simultaneously. For the signal reaction, we have calculated the matrix element squared of the process $pp \rightarrow Q\bar{Q}$ with *polarized* final state quarks and incorporated the exchange, including the t -channel contributions, of all the SM gauge bosons as well as their KK excitations and those of the Z' boson. For the background processes, the contributions of both the $q\bar{q}$ and gg initial states have been calculated and the exchange of the KK excitations of the gauge bosons were switched off. To obtain the cross sections σ at the hadronic level, we use the CTEQ5M1 set of parton distributions [34] with the factorization and a renormalization scales set to the invariant mass of the $Q\bar{Q}$ system, $\mu_F = \mu_R = m_{Q\bar{Q}}/2$.

The significance \mathcal{S} of the signal in the RS model can be then defined as

$$\mathcal{S}_{\mathcal{L}} = \frac{\sigma^{\text{RS+SM}} - \sigma^{\text{SM}}}{\sqrt{\sigma^{\text{SM}}}} \times \sqrt{\mathcal{L}}, \quad (4)$$

where \mathcal{L} denotes the total integrated LHC luminosity. In our analysis, we will chose two examples for the luminosity: a lower value $\mathcal{L} = 10 \text{ fb}^{-1}$ that is expected in the first years of the LHC running and a high value $\mathcal{L} = 100 \text{ fb}^{-1}$ which is expected to be reached after a few years of running.

In order to enhance the signal, which is peaked at the invariant mass of the $Q\bar{Q}$ system (as will shown in details later), and to suppress the continuum background, one needs to select events near the KK resonance. Throughout this analysis, we impose a cut on the invariant mass of the $Q\bar{Q}$ final state

$$|m_{Q\bar{Q}} - M_{KK}| \leq \Gamma_{V_{KK}} \quad (5)$$

To further reduce the backgrounds, we also impose the following cuts on the transverse momenta of the two final jets and their rapidity

$$p_T^{Q,\bar{Q}} \geq 200 \text{ GeV} , |\eta_{Q,\bar{Q}}| \leq 2 \quad (6)$$

as in the signal, the p_T of the jets is peaked close to $\frac{1}{2}M_{V_{\text{KK}}}$ and the production is central, while in the background, the jets are peaked in the forward and backward directions and the bulk of the cross section is for low p_T jets. These cuts can certainly be improved to optimize the signal to background ratio but we will refrain from performing such an optimization here. In fact, in this preliminary and simple parton-level investigation, we will simply compare the signal and the main corresponding physical background to determine if, grossly, the exchanges of the KK states could give rise to a promising and possibly detectable signal. A more detailed Monte-Carlo study, including precise experimental effects, initial and final state radiation, the correct identification of the t/b states and the measurement of their momenta, more efficient and realistic cuts and detection efficiencies, which is beyond our scope here, will be needed. Nevertheless, the large significances that we will present are expected to remain at an interesting level after implementation of these experimental effects.

3.2 The cross sections

The invariant mass distributions $d\sigma/dm_{t\bar{t}}$ of the process $pp \rightarrow t\bar{t}$, are shown in Fig. 2 for the four scenarios E_1 to E_4 ; the cuts on the transverse momenta and the rapidity of the final t -jets given in eq. (6) have been applied. Shown are the distributions in the case of the SM background, $qq/gg \rightarrow t\bar{t}$, in the case where the KK excitation of the gluon is also exchanged, $q\bar{q} \rightarrow g, g^{(1)} \rightarrow t\bar{t}$, and in the case where all the KK excitations of the electroweak gauge bosons are also exchanged $q\bar{q} \rightarrow g, g^{(1)}, \gamma^{(1)}, Z^{(1)}, Z'^{(1)} \rightarrow t\bar{t}$. As already mentioned, we have used a common mass for the KK gauge bosons, $M_{\text{KK}} = 3 \text{ TeV}$, with the couplings given in Table 1 that lead to the $b\bar{b}, t\bar{t}$ branching ratios and total decay widths displayed in Table 2.

As can be seen from the figure, there is a substantial contribution of the KK excitations to the invariant mass distribution, in particular around the peak $m_{t\bar{t}} \sim 3 \text{ TeV}$. At higher invariant masses the KK contribution becomes small, while at invariant masses lower than M_{KK} it is significant even for $m_{t\bar{t}} \sim 2 \text{ TeV}$; only for $m_{t\bar{t}} \lesssim 1 \text{ TeV}$ the KK contribution becomes negligible. Outside the KK mass peak, the RS effect is mostly due to the interference between the excited state and SM contributions; this interference is positive below and negative above the peak [where the real part of the propagator of the KK state changes sign]. The dominant contribution compared to the SM case is by far due to the exchange of the excitation of the strongly interacting gluon which has the largest (QCD versus EW) couplings to the initial state partons. The contributions of the KK photon and KK Z boson increase the peak only slightly. In turn, the KK excitation of the Z' boson has a negligible impact on $t\bar{t}$ production

as it does not couple to the initial light quarks, $Q'(c_{\text{light}}) = 0$, and the parton density of the heavier bottom quark in the proton is small.

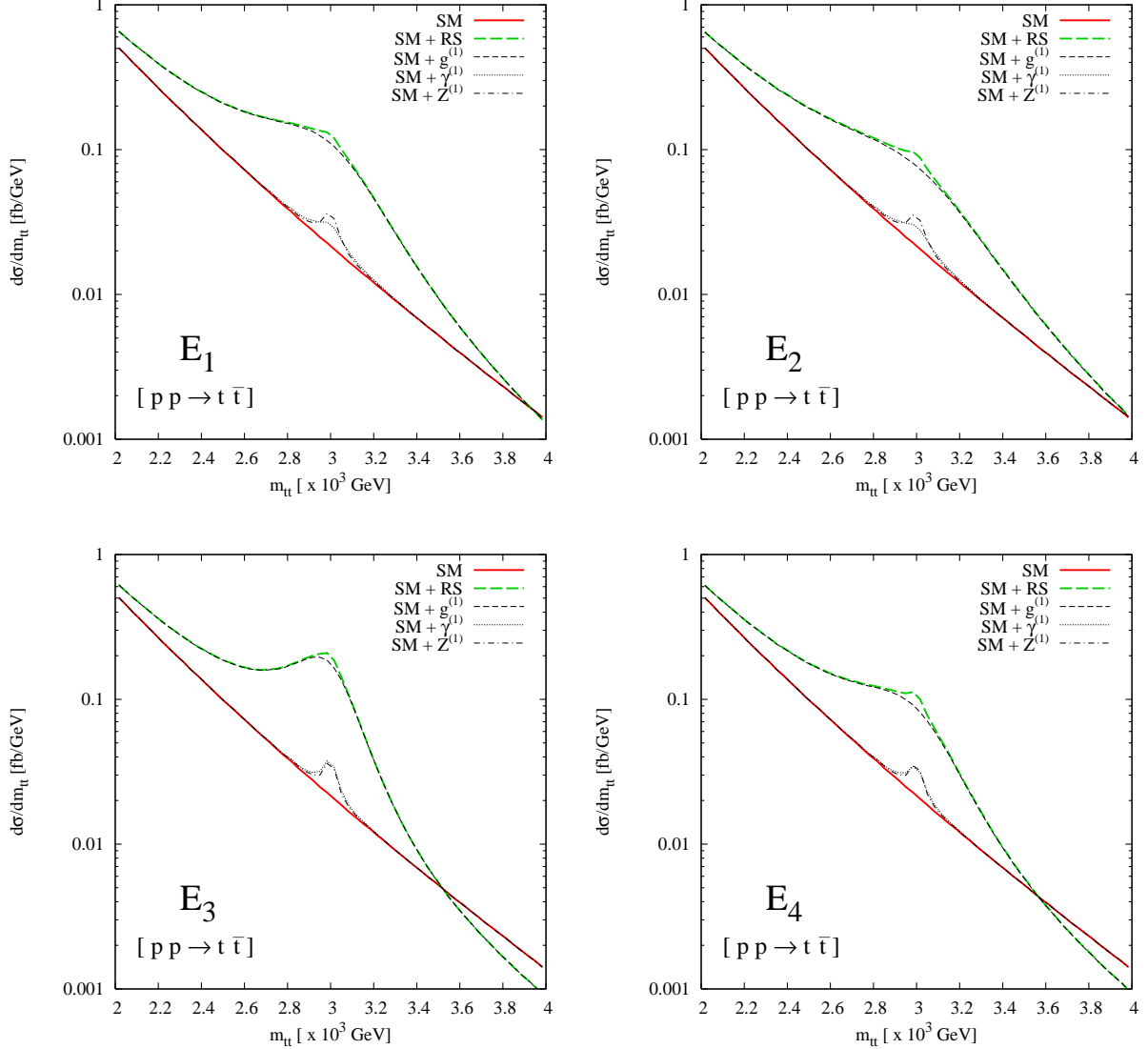


Figure 2: The invariant mass distribution of the cross section for the $pp \rightarrow t\bar{t}$ process for all four scenarios $E_{1,2,3,4}$ defined in Table 1. We use the CTEQ5M1 set of parton distribution functions and include the cuts of eq. (6) on the $p_T^{t,\bar{t}}$ and $\eta_{t,\bar{t}}$ of the final quarks. The solid curve is for the SM background and the long-dashed one for the RS model with contributions of all the first KK excitations of the gauge bosons $g^{(1)}$, $\gamma^{(1)}$, $Z^{(1)}$ included; the short-dashed curve is for the SM case along with only $g^{(1)}$ exchange; the dotted curve is for the SM case along with only $\gamma^{(1)}$ exchange; the dashed-dotted curve is for the SM case along with only $Z^{(1)}$ exchange.

The total cross sections of the $pp \rightarrow t\bar{t}$ process are displayed in Table 3 first for the SM background only and then in the RS model in which all contributions of the KK excitations

	SM	SM+RS	$\mathcal{S}_{10}^{\text{RS}}$	$\mathcal{S}_{100}^{\text{RS}}$	$\mathcal{S}_{100}^{g^{(1)}}$	$\mathcal{S}_{100}^{\gamma^{(1)}}$	$\mathcal{S}_{100}^{Z^{(1)}}$
E_1	47.0	135	41	128	124	5.7	7.4
E_2	90.5	181	30	95	91	5.2	7.0
E_3	16.6	83.4	52	164	157	7.8	7.0
E_4	34.1	88.7	30	94	88	6.4	6.4

Table 3: Left: The $pp \rightarrow t\bar{t}$ cross sections [in fb] in the SM and in the RS model with the exchange of all the KK excitations as well as the significance of the signal for $\mathcal{L} = 10 \text{ fb}^{-1}$ and $\mathcal{L} = 100 \text{ fb}^{-1}$. Right: the significance for $\mathcal{L} = 100 \text{ fb}^{-1}$ of the signal when only the separate contributions of the KK excitations of the gluon, photon and Z bosons are added to the SM contribution. These numbers are obtained after the cuts of eqs. (5) and (6) are applied.

[gluon, photon and Z boson] are added; the cuts on the invariant mass, transverse momentum and rapidity of the t and \bar{t} jets, eqs. (5) and (6), are applied. The significance of the full signal with a common mass, $M_{\text{KK}} = 3 \text{ TeV}$, is also shown for the integrated luminosities $\mathcal{L} = 10$ and 100 fb^{-1} . As can be seen, the significance of the excess of events in the RS scenarios when all KK excitations are included is large in the four cases, $\mathcal{S}_{10}^{\text{RS}} \gtrsim 30$ for a moderate luminosity and $\mathcal{S}_{100}^{\text{RS}} \gtrsim 90$ for an high luminosity.

To illustrate the impact of each KK state separately, the right-hand side of Tab. 3 shows the significance of the signal in the case where only one KK excitation is exchanged in the $pp \rightarrow t\bar{t}$ process, that is, when the mass of the two other excitations is (artificially) set to high values. As one might have expected, since the excess over the SM background is mainly due to the exchange of the KK gluon, the significance in this case, $\mathcal{S}_{100}^{g^{(1)}}$, is almost the same as when the full signal is considered, $\mathcal{S}_{100}^{\text{RS}}$. In the case where only the first KK excitation of the photon or the Z boson is considered, the significance is much smaller. This is a mere consequence of the fact that the electroweak couplings of the $\gamma^{(1)}, Z^{(1)}$ bosons are much smaller than the QCD couplings of the $g^{(1)}$, leading to limited production cross sections. The smaller rates are, however, partly compensated by the smaller total decay widths and one obtains in some scenarios significance at high luminosities that are large enough for the effects to be detectable at the LHC, $\mathcal{S}_{100}^{\gamma^{(1)}, Z^{(1)}} \gtrsim 5$.

The significance of the signal strongly depends on the chosen scenario which fixes the couplings of the KK excitations to the t, b quarks. If the couplings to top quarks are large, the $pp \rightarrow V_{\text{KK}} \rightarrow t\bar{t}$ production rate is substantial but the total decay width is also large leading to a more diluted signal. The signal is even more diluted when the couplings of the KK excitations to b quarks is at the same time large: on the one hand, this increases the total decay width of the excitation and, on the other hand, it lowers the branching ratio into the $t\bar{t}$ final states that we are looking at. Taking the example of the $g^{(1)}$ state,

the best significance is obtained in scenario E_3 in which the couplings to the b quarks are not too strongly enhanced (see Table 1) so that the $g^{(1)}$ total decay width is the smallest, $\Gamma_{g^{(1)}} \simeq 330$ GeV (see Table 2), and the branching ratio for decays into top quarks is among the largest ones, $\text{BR}(g^{(1)} \rightarrow t\bar{t}) \simeq 83\%$. In scenario E_1 , where the parameters are as in scenario E_3 except for the $Q(c_{t_R})$ and $Q'(c_{t_R})$ charges which are larger, the total decay width of $g^{(1)}$ doubles, $\Gamma_{g^{(1)}} \simeq 630$ GeV, while the fraction for decays into top quarks is not significantly affected, $\text{BR}(g^{(1)} \rightarrow t\bar{t}) \sim 91\%$, leading to a smaller significance, $\mathcal{S}_{10}^{\text{RS}} = 41$ versus $\mathcal{S}_{10}^{\text{RS}} = 52$. In scenarios E_2 and E_4 , the total decay widths of $g^{(1)}$ are larger and the $t\bar{t}$ branching ratios smaller so that the significance of the signals is reduced compared to the two previous scenarios.

The discussion for the production process $pp \rightarrow b\bar{b}$ is quite similar to that of $pp \rightarrow t\bar{t}$ except for the fact that the t -channel contribution to the $b\bar{b} \rightarrow b\bar{b}$ subprocess has to be added. The smallness of the parton distribution function of the bottom quark can be partly compensated by the potentially larger KK gauge couplings of the $b_{L,R}$ states [for small c_{b_R} values as shown in Table 1] compared to light quarks. For instance, this $b\bar{b}$ contribution reaches the level of $\sim 10\%$ in the SM+RS cross section in scenario E_4 . However, this contribution does not peak at a given invariant mass value. The invariant mass distribution $d\sigma/dm_{b\bar{b}}$ for bottom quark pair production is shown in Fig. 3 for $m_{b\bar{b}}$ between 2 and 4 TeV. As previously, the cuts on the transverse momenta and rapidity of the final jets given in eq. (6) have been applied. Here, we simply show the SM background and the signal excess in the case where the contributions of all KK excitations are simultaneously included; again, this excess is largely dominated by the exchange of the KK excitation of the gluon.

The signals are less striking than in the $pp \rightarrow t\bar{t}$ case, the main reason being due to the fact that the branching ratios $\text{BR}(g^{(1)} \rightarrow b\bar{b})$ are much smaller than $\text{BR}(g^{(1)} \rightarrow t\bar{t})$, due to the hierarchy between the b and t couplings (see Table 1), except in scenario E_4 and, to a lesser extent scenario E_2 , in which they are comparable. The cross section in the SM and in the RS model, as well as the significance of the signal for the two possible luminosities $\mathcal{L} = 10$ and 100 fb^{-1} , are shown in Table 4 in the four scenarios when the cuts of eqs. (5) and (6) are applied. One can see that in all cases the significance is large enough, $\mathcal{S}_{10}^{\text{RS}} \gtrsim 5$, to allow for the detection of the signal even at moderate luminosities. For example, in the parameter set E_4 , the c_{b_R} value is smaller than for E_3 so that the KK gauge coupling to b is larger, leading to higher $b\bar{b}$ production cross section and significance. Comparing now E_4 to E_2 , c_{t_R} is larger which induces smaller widths for KK gauge bosons and thus a better significance, for same reasons as before.

Note that when combining the $pp \rightarrow t\bar{t}$ and $pp \rightarrow b\bar{b}$ processes, one would in principle be able to have access to the couplings of the KK states $g^{(1)}$ to top and bottom quarks. However, it would have only a small contamination from the various overlapping electroweak KK resonances, since the major part of the signal is due to the contribution of the gluon

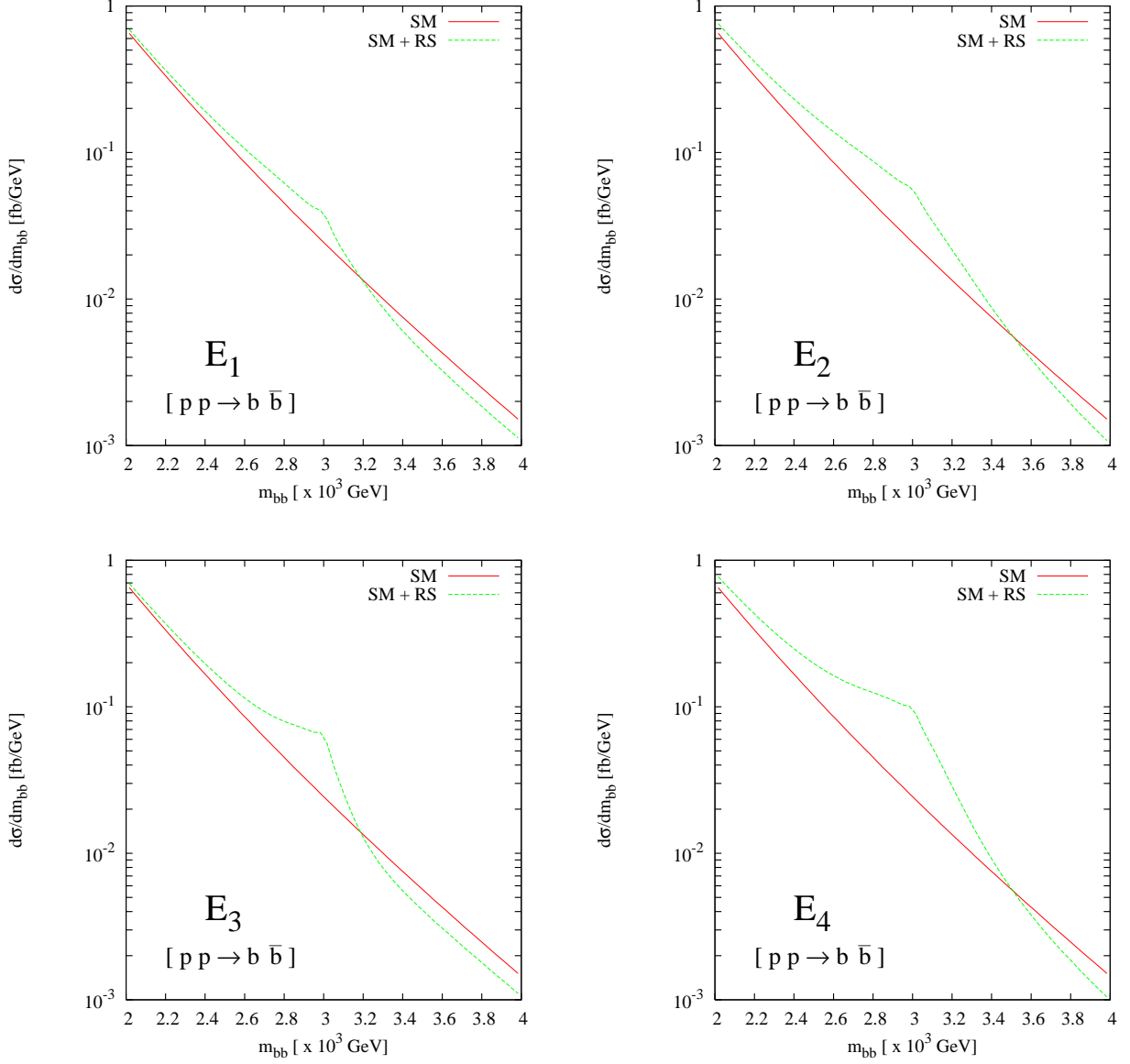


Figure 3: The invariant mass distribution of the cross section for the $pp \rightarrow b\bar{b}$ process for all four parameter sets $E_{1,2,3,4}$ defined in Table 1. We use the CTEQ5M1 set of parton distribution functions and include the cuts of eq. (6) on the $p_T^{b,\bar{b}}$ and $\eta_{b,\bar{b}}$ of the final quarks. The solid curve is for the SM background and the long-dashed one for the RS model with contributions of all the first KK excitations of the gauge bosons $g^{(1)}, \gamma^{(1)}, Z^{(1)}, Z'^{(1)}$ included.

excitation. As the couplings are parity violating, an additional and important information is provided by some polarization and forward-backward asymmetries to which we turn our attention now.

	SM	SM+RS	$\mathcal{S}_{10}^{\text{RS}}$	$\mathcal{S}_{100}^{\text{RS}}$
E_1	55.3	67.6	5.2	17
E_2	109	159	15	48
E_3	17.0	32.8	12	38
E_4	39.7	90.0	25	80

Table 4: The $pp \rightarrow b\bar{b}$ cross sections [in fb] in the SM and in the RS model with the exchange of all the KK excitations as well as the significance of the signal for $\mathcal{L} = 10 \text{ fb}^{-1}$ and $\mathcal{L} = 100 \text{ fb}^{-1}$; the cuts of eqs. (5) and (6) have been applied.

3.3 Polarization and forward–backward asymmetries

Each of the KK excitations of the gauge bosons, $g^{(1)}$, $\gamma^{(1)}$ and $Z^{(1)}$, has a different coupling to the right– and left–handed top quarks [which are themselves different from the SM ones]. These couplings appear in the forward–backward asymmetry as well as in the polarization of the produced top quarks. While the enhancement in the production rate due to a single KK gauge boson is proportional to the sum of squared couplings $(g_{Q_L}^{V_{\text{KK}}})^2 + (g_{Q_R}^{V_{\text{KK}}})^2$, the polarization and forward–backward asymmetries are proportional to the difference $(g_{Q_L}^{V_{\text{KK}}})^2 - (g_{Q_R}^{V_{\text{KK}}})^2$. Thus, a combined measurement of the cross section together with asymmetries would determine the couplings of the vector boson V_{KK} . However, since the process is mediated by the exchange of several KK gauge bosons with differing right– and left–handed couplings, it will not be possible to measure these couplings for any of the electroweak KK excitations. This is particularly true as the major contribution to the total rate for $\sigma(pp \rightarrow Q\bar{Q})$ is coming from $g^{(1)}$, as the contribution from the electroweak excitations $\gamma^{(1)}$, $Z^{(1)}$ and $Z'^{(1)}$ is relatively small. Nevertheless, the measurement of the polarization and forward–backward asymmetries for top quarks, on which we will concentrate here, will be instrumental in establishing the presence of parity violating KK gauge bosons.

The polarization of the produced top quarks is defined as:

$$P_t = \frac{N_R - N_L}{N_R + N_L}, \quad (7)$$

where N_R and N_L are the numbers of events with right– and left–handed helicity for the top quark with a given set of kinematical cuts⁹. The statistical error in the measurement of this

⁹We note here that even for extra–dimensional models in which the KK excitations have the same couplings as their SM counterparts, the $Z^{(1)}$ state will always have parity violating couplings and hence, the produced top quarks will be polarized. However, in this case, following the structure of the SM, the left chiral top quark has larger coupling to the $Z^{(1)}$ excitation, leading to a negative polarization. On the other hand, in the RS model that we consider here, the right chiral top quarks have larger couplings to the KK gauge bosons, leading to a positive polarization.

polarization, in terms of the rate σ and the LHC luminosity \mathcal{L} , is given by

$$\Delta P_t = \frac{1}{\sqrt{N_R + N_L}} \sqrt{1 - P_t^2} = \frac{1}{\sqrt{\sigma \times \mathcal{L}}} \sqrt{1 - P_t^2}, \quad (8)$$

The polarization of the top quark is shown in Fig. 4 in the case of the SM and for the RS scenario E_1 as a function of the invariant mass $m_{t\bar{t}}$; again the cuts of eqs. (6) have been applied and the contributions of all virtual KK states has been included.

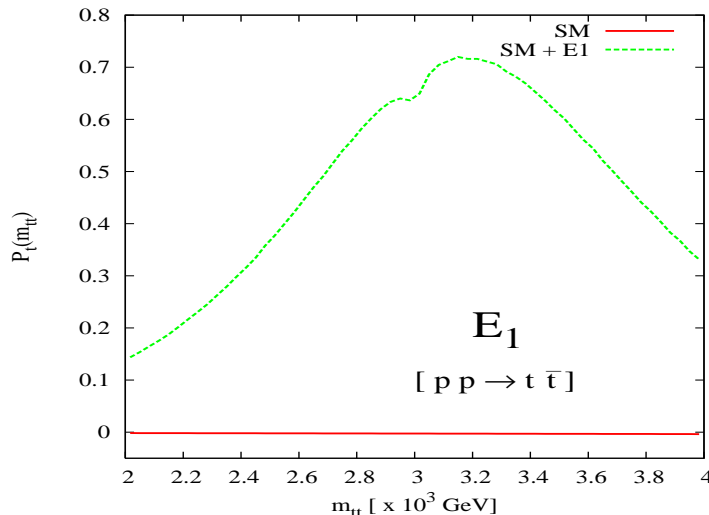


Figure 4: The top quark polarization as a function of the invariant mass $m_{t\bar{t}}$ in the reaction $pp \rightarrow t\bar{t}$ in the SM (solid) and in the RS model (dashed) for the set E_1 of parameters.

The polarization is a parity odd quantity and can assume a non-zero value only in the presence of parity violating interactions. In the SM case, the only source of parity violation is the contribution of the Z boson, which leads to a small negative polarization of order $\sim 10^{-3}$. The dominant contribution for $m_{t\bar{t}}$ near M_{KK} is due to $g^{(1)}$ which has a larger coupling to t_R than to t_L in the chosen RS scenarios; this leads to a large polarization roughly of the size

$$\frac{(g_{t_R}^{V_{KK}})^2 - (g_{t_L}^{V_{KK}})^2}{(g_{t_R}^{V_{KK}})^2 + (g_{t_L}^{V_{KK}})^2} \equiv G_{-+}^{V_{KK}} \quad (9)$$

coming from the $q\bar{q}$ fusion channel. However, there is a dilution of this polarization due to the parity-conserving SM production of top pairs through gg fusion and $q\bar{q}$ annihilation with gluon exchange. For instance, in the case of scenario E_1 , one has for the first gluon excitation $g^{(1)}$, $G_{-+}^{g^{(1)}} = 0.86$, while the degree of polarization, $P_t = 0.505$, is diluted by the SM QCD processes. Similar results are obtained in the other scenarios and one has: $P_t \simeq 0.37, 0.52, 0.38$ in scenarios E_2, E_3, E_4 , respectively. Furthermore, there is some subleading contribution from the $\gamma^{(1)}$ and $Z^{(1)}$ states which is, for instance, visible as a small “dip” just before the peak in the $m_{t\bar{t}}$ distribution of the polarization P_t in Fig. 4.

The polarization of the top quark is not a direct observable. Nevertheless, it is reflected for instance in the angular distribution of the lepton coming from the decaying top quark, $t \rightarrow bW \rightarrow b\ell\nu$ with $\ell = e, \mu$. In the rest frame of the t -quark, the leptons issued from these decays are isotropically distributed for unpolarized top quarks. For positive P_t , the lepton distribution is peaked in the direction of the “would be” boost or the direction of quantization axis, and for negatively polarized top quarks, the peak is in the opposite direction. In the laboratory frame, the decay products of the fast moving top quark are collimated in the forward direction due to the boost. Thus, for the positively polarized top quarks, there will be additional focusing of the leptons in the direction of the top quark momenta. Accordingly, there is a de-focusing of the lepton distribution for the negatively polarized top quarks. Thus, the simplest quantity to look at is the azimuthal distribution (or the focusing) of the leptons with respect to the top production plane [35]. We thus define the following asymmetry in the laboratory frame:

$$A_\ell = \frac{\sigma(\cos \phi_\ell > 0) - \sigma(\cos \phi_\ell < 0)}{\sigma(\cos \phi_\ell > 0) + \sigma(\cos \phi_\ell < 0)}, \quad (10)$$

where ϕ_ℓ is the azimuthal angle of the decay leptons with respect to the t -quark production plane, or with respect to the transverse momentum of the top quark. Again, the statistical error in the measurement of the asymmetry and the corresponding significance is given by

$$\Delta A_\ell = \frac{1}{\sqrt{\sigma \times \mathcal{L}}} \sqrt{1 - A_\ell^2} \quad \text{and} \quad \mathcal{S} = \frac{A_\ell^{RS+SM} - A_\ell^{SM}}{\Delta A_\ell^{SM}} \quad (11)$$

respectively. The values of the asymmetries in the various RS scenarios and the significance in their measurements are shown in the right-hand side of Table 5.

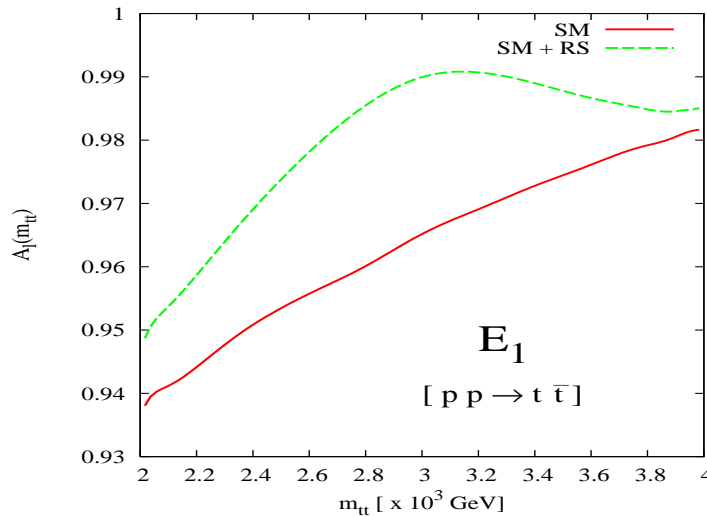


Figure 5: The lepton asymmetry distribution versus the $m_{t\bar{t}}$ invariant mass for the process $pp \rightarrow t\bar{t}$ in SM and in the RS scenario E_1 .

Since we are dealing with heavy KK bosons, the top quarks are highly boosted in the center of mass frame, which leads to highly collimated decay products even for unpolarized top quarks. This explains the large value of the asymmetry, $A_\ell \simeq 0.96$, for the SM in the case of E_1 cuts for example; see Table 5. A modification of the top polarization changes the collimation of the decay products and, thus, affects this SM asymmetry. For instance, again in scenario E_1 , one expects a large and positive polarization for the top quarks, which leads to a slightly larger asymmetry value, $A_\ell \simeq 0.98$. The significance \mathcal{S} calculated according to eq. (11), indicates that this asymmetry should be observable at the LHC but only for a high luminosity run in a post-discovery analysis [the discovery being clearly possible at a low luminosity] as shown in Table 5. Therefore, the associated distribution displayed in Fig. 5 for the parameter set E_1 , which exhibits a specific shape, should help in identifying the RS scenario. In particular, the fact that this A_ℓ asymmetry is enhanced by the RS contribution proves that the exchanged KK gauge bosons couple effectively more to the t_R than to the t_L state.

	A_ℓ^{SM}	$A_\ell^{\text{RS+SM}}$	$\mathcal{S}_{10}^{A_\ell}$	$\mathcal{S}_{100}^{A_\ell}$	$A_{\text{FB}}^{\text{SM}}$	$A_{\text{FB}}^{\text{RS+SM}}$	$\mathcal{S}_{10}^{A_{\text{FB}}}$	$\mathcal{S}_{100}^{A_{\text{FB}}}$
E_1	0.957	0.982	1.5	4.7	-0.00178	0.195	7.2	23
E_2	0.952	0.972	1.3	4.1	0.00737	0.157	6.7	21
E_3	0.963	0.987	1.2	3.8	-0.00666	0.232	6.7	21
E_4	0.960	0.980	1.0	3.2	-0.00407	0.181	5.4	17

Table 5: Left: The polarization and forward–backward asymmetries, A_ℓ and A_{FB}^t , for the process $pp \rightarrow t\bar{t}$ in the SM and in the RS model with the exchange of all the KK excitations as well as the significance of their measurements for $\mathcal{L} = 10 \text{ fb}^{-1}$ and $\mathcal{L} = 100 \text{ fb}^{-1}$.

Let us now turn our attention to the forward–backward asymmetry. The s -channel diagrams exchanging gauge bosons with parity violating couplings lead to a forward–backward asymmetry in the top quark pair production in the center of mass frame with respect to the quark direction. However, since at the LHC there are two identical protons colliding, there is no simple forward–backward asymmetry in the laboratory frame due to the symmetric distribution of the initial state quarks and anti-quarks. But, since the proton is mainly composed of quarks and with only a small proportion of anti-quarks in the sea, the fusing $q\bar{q}$ pairs are highly boosted in the laboratory frame, mainly in the direction of the incoming quarks. Thus, one can construct a kind of forward–backward asymmetry with respect to the direction of the boost in the center of mass frame. In the laboratory frame, we first arbitrarily label the proton beams as “1” and “2”, and then define a quantity

$$C = \left(\frac{x_1 - x_2}{x_1 + x_2} \right) \cos \theta_t^{\text{lab}} \quad (12)$$

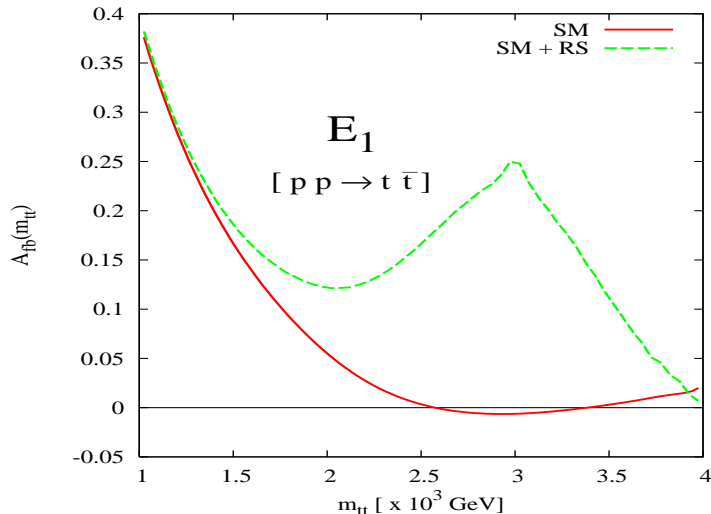


Figure 6: The forward–backward asymmetry distribution versus the invariant mass $m_{t\bar{t}}$ for the reaction $pp \rightarrow t\bar{t}$ in the SM and in the RS scenario E_1 .

where x_i are the momenta fractions of the colliding partons and θ_t^{lab} the t -quark polar angle with respect to the beam “1”; the quantity in the brackets is the boost of the center of mass frame in the laboratory frame. With respect to this quantity we define a forward–backward asymmetry with respect to the direction of boost:

$$A_{\text{FB}}^t = \frac{\sigma(C > 0) - \sigma(C < 0)}{\sigma(C > 0) + \sigma(C < 0)}. \quad (13)$$

This quantity is closely related to the forward–backward asymmetry in the center of mass frame, with respect to the quark direction, up to some smearing due to the boost of the center of mass frame and possible misidentification of a \bar{q} as a q for a faster moving \bar{q} . The statistical error in the measurement of this asymmetry is given by

$$\Delta A_{\text{FB}}^t = \frac{1}{\sqrt{\sigma \times \mathcal{L}}} \sqrt{1 - (A_{\text{FB}}^t)^2}. \quad (14)$$

We should note that the above asymmetry is not a pure probe of parity violation, i.e. it can be non–zero and positive even for parity–conserving processes. The reason is the boost of the center of mass frame with respect to the quark direction, which leads to focusing of particles in the forward direction. This explains the large value of A_{FB}^t for the SM as shown in Fig. 6 by a solid line. Additional sources of a forward–backward asymmetry in the center of mass frame change the value of A_{FB}^t , which is shown in Fig. 6 by a dashed line for the RS scenario E_1 where there is a significant contribution from parity violating couplings of the $g^{(1)}$ excitation. Once more, there is some finite contribution from the electroweak KK modes which appears as a “nipple” peak in the $m_{t\bar{t}}$ distribution of A_{FB}^t , Fig. 6.

The obtained values of A_{FB}^t and their significance given in Table 5 for all scenarios, shows that it is potentially visible at the LHC even at low luminosity with $\mathcal{S}_{10}^{A_{\text{FB}}^t} \geq 5$. Such significant shifts in the asymmetry with respect to the SM expectation would strongly indicate parity violation in the top couplings to KK gauge bosons. Indeed, these typical asymmetry deviations cannot be entirely explained by interferences between hypothetical parity-conserving bosons and the parity violating SM Z boson. Moreover, the profile of the A_{FB}^t distribution in Fig. 6 is characteristic of the exchange of several KK gauge bosons. The enhancement of A_{FB}^t originates from the fact that the effective couplings of KK gauge bosons, and mainly the KK gluon $g^{(1)}$, are larger for the t_R than for t_L .

Note that we have also calculated the asymmetry A_{FB}^b for the $pp \rightarrow b\bar{b}$ production process, but we do not present the corresponding results as the significance is rather low in all the considered scenarios. Furthermore, we will not discuss the polarization of the produced bottom quarks as it will not be experimentally measurable.

4. The higher order processes

4.1 The gluon–gluon fusion mechanism

The higher order gluon–gluon fusion contribution to the heavy quark pair production at LHC, via KK gauge boson exchange, should be favored by the large V_{KK} couplings to heavy quarks. Such a reaction occurs through a loop involving mainly the heavy top and bottom quarks and a V_{KK} exchanged in the s-channel, as shown in Fig. 7(a). Indeed, the main reaction is via $V_{KK} = g^{(1)}$ which receives no contributions from the light quarks in the loop as those have quasi identical $g^{(1)}$ couplings for the left and right chirality (fixed by a common $Q^{(l)}(c_{light})$ value as explained at the end of Section 2.2) which makes the final amplitude vanishing. This reaction represents the dominant two–body production mechanism for KK excitations which do not couple to light quarks.

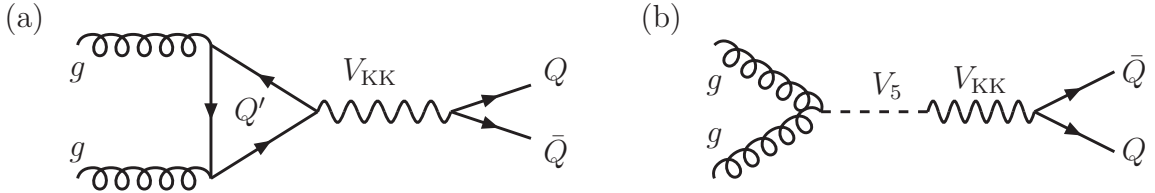


Figure 7: *The Feynman diagram for $Q\bar{Q}$ ($Q = b, t$) production, via V_{KK} exchange, at the LHC through the quark loop induced gluon-gluon fusion process (a) and the counter-term with the Stückelberg mixing that regulates the gauge anomaly of the ggV_{KK} vertex (b).*

The effective one–loop vertex $g(k_1^\nu)g(k_2^\rho)V_{KK}(k_3^\mu)$, where $k_1^\nu, k_2^\rho, k_3^\mu$ denote the respective momenta (k_1 and k_2 being taken as incoming with respect to the flow in the loop), is given

in momentum space by,

$$\Gamma_{\mu\nu\rho}^{ijk} = t^{ijk} \left[\left(A_1(k_1, k_2) - B_2(k_1, k_2) \right) \epsilon_{\mu\nu\rho\sigma} (k_1^\sigma - k_2^\sigma) + \frac{B_1(k_1, k_2)}{2k_1 \cdot k_2} k_2^\sigma k_1^\tau (k_2^\nu \epsilon_{\mu\rho\sigma\tau} - k_1^\rho \epsilon_{\mu\nu\sigma\tau}) \right], \quad (15)$$

with,

$$t^{ijk} = g_s^2 \text{Tr}[\lambda_i \lambda_j \lambda_k] \sum_f \left[g_{q_L}^V Q^{(f)}(c_{q_L}) - g_{q_R}^V Q^{(f)}(c_{q_R}) \right], \quad (16)$$

g_s being the strong interaction coupling constant, λ_i [$i = 1, \dots, 8$] the Gell-Mann matrices (only two such matrices must be taken in the case of colorless KK excitations: $V_{KK} \neq g^{(1)}$), $\epsilon_{\mu\nu\rho\sigma}$ the purely antisymmetric tensor and $q_{L/R}$ the quarks running in the loop. Finally, the $A_1(k_1, k_2)$ function, entering eq. (15), represents the usual amplitude a priori divergent. The finite functions $B_{1,2}(k_1, k_2)$ are defined later.

Indeed, the amplitude eq. (15) contains an anomaly in the third current. As a matter of fact, only two of the three Ward identities that the vertex must obey are satisfied¹⁰:

$$\begin{aligned} k_1^\nu \Gamma_{\mu\nu\rho}^{ijk} &= 0, & k_2^\rho \Gamma_{\mu\nu\rho}^{ijk} &= 0, \\ -k_3^\mu \Gamma_{\mu\nu\rho}^{ijk} &= -(k_1^\mu + k_2^\mu) \Gamma_{\mu\nu\rho}^{ijk} = -t^{ijk} 2(A_1(k_1, k_2) - B_2(k_1, k_2)) \epsilon_{\nu\rho\sigma\tau} k_2^\sigma k_1^\tau. \end{aligned} \quad (17)$$

The first two relations allow to define the ambiguous amplitude $A_1(k_1, k_2)$ in terms of finite functions:

$$A_1(k_1, k_2) - B_2(k_1, k_2) - \frac{B_1(k_1, k_2)}{2} = 0. \quad (18)$$

However, the ggV_{KK} vertex receives another contribution from the exchange of the gauge field fifth component V_5 , as drawn in Fig. 7(b). There, the ggV_5 coupling originates from the so-called Chern–Simons term in the action (see Ref. [38] for the case of warped orbifolds) which can be written in terms of the gauge covariant field strengths as [39, 40]:

$$S_{CS} = \int d^4x dy \rho(y) \epsilon^{MNPQR} \text{Tr} \left[A_M F_{NP} F_{QR} + i A_M A_N A_P F_{QR} - \frac{2}{5} A_M A_N A_P A_Q A_R \right], \quad (19)$$

where the Roman letter indices M, N, \dots run over all dimensions. While the mixing between $\partial_\mu A_5^{(n)}$ and $A_\mu^{(n)}$ (the Greek letter index μ is running over the first four dimensions only), appearing in the diagram of Fig. 7(b), and proportional to the gauge KK mass, comes from the Stückelberg term; see for instance Refs. [39, 41]. Following Ref. [41], one finds that the diagram of Fig. 7(b) gives rise to a vertex contribution of the form,

$$\Gamma_{\mu\nu\rho}^{ijk}|_{CS} = 2t^{ijk} A_1(k_1, k_2) \frac{k_{1\mu} + k_{2\mu}}{(k_1 + k_2)^2} \epsilon_{\nu\rho\sigma\tau} k_2^\sigma k_1^\tau. \quad (20)$$

The whole amplitude is then free from any gauge anomaly as one has now,

$$k_1^\nu (\Gamma_{\mu\nu\rho}^{ijk} + \Gamma_{\mu\nu\rho}^{ijk}|_{CS}) = 0, \quad k_2^\rho (\Gamma_{\mu\nu\rho}^{ijk} + \Gamma_{\mu\nu\rho}^{ijk}|_{CS}) = 0,$$

¹⁰See Ref. [36, 37] for the generic computations of gauge anomalies in the context of S^1/\mathbb{Z}_2 orbifold models.

$$-k_3^\mu (\Gamma_{\mu\nu\rho}^{ijk} + \Gamma_{\mu\nu\rho}^{ijk}|_{CS}) = 2t^{ijk} B_2(k_1, k_2) \epsilon_{\nu\rho\sigma\tau} k_2^\sigma k_1^\tau, \quad (21)$$

where B_2 is proportional to the mass of fermions running in the loop. Therefore, as expected, there is a mechanism responsible for the cancellation of the gauge anomaly.

The B functions entering above equations read as,

$$B_1(k_1, k_2) = \frac{2}{3(2\pi)^2} \int_0^1 dz \int_0^{1-z} dx \frac{x(x+z-1)}{(m_f^2/(2k_1 \cdot k_2)) - xz},$$

$$B_2(k_1, k_2) = \frac{2}{3(2\pi)^2} \int_0^1 dz \int_0^{1-z} dx \frac{(1-z)m_f^2}{m_f^2 - (2k_1 \cdot k_2)xz}, \quad (22)$$

In conclusion, both the vertex contributions eq. (15) and eq. (20) have to be taken into account in the calculation of the quark contribution to the ggV_{KK} vertex. Note that the correction eq. (20) vanishes in the on-shell regime limit for V_{KK} where $k_3^\mu \epsilon_{3\mu} = 0$, ϵ_3 being its polarization vector. This is consistent with Yang's theorem according to which the entire production cross section vanishes if the two initial zero-mode gluons as well as the produced KK gauge boson are simultaneously on-shell. This is illustrated by the $m_{t\bar{t}}$ invariant mass distribution that we will discuss now.

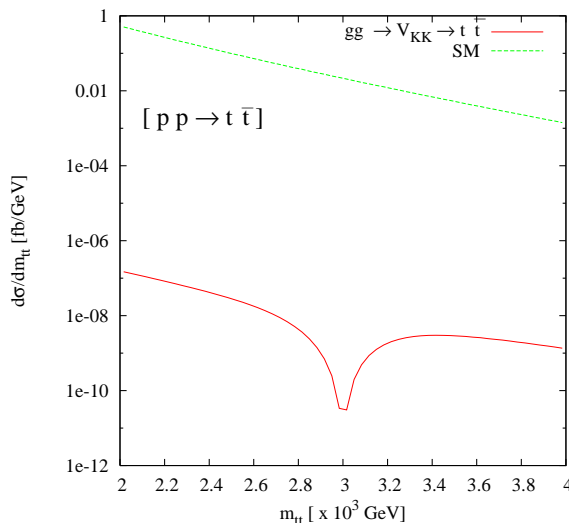


Figure 8: The $m_{t\bar{t}}$ distribution of the cross-section corresponding to the reaction shown in Fig. 7 for $V_{KK} = g^{(1)}$ for the E_2 choice of parameters. The whole SM distribution is also shown for comparison.

The $m_{t\bar{t}}$ distribution for the above said process is shown in Fig. 8, along with that for the SM background, for the excitation $g^{(1)}$ and the E_2 choice of RS parameters. The dip in the distribution near the mass $m_{t\bar{t}} = m_{KK}$ is due to the vanishing coupling for on-shell V_{KK} bosons with a pair of gluons. The shape of the distribution depends upon the total decay

width of the V_{KK} . However, the rates for the signals are several orders of magnitude smaller than the SM background. The cross sections are even smaller for the KK excitations of the electroweak gauge bosons. One can then conclude that the gluon–gluon fusion mechanism for the production of KK excitations will not be relevant at the LHC.

4.2 Associated production with heavy quarks

In this section, we briefly discuss the associated production of the KK excitations of the gauge bosons with heavy quarks

$$gg/q\bar{q} \rightarrow Q'\bar{Q}' V_{\text{KK}} \rightarrow Q'\bar{Q}' Q\bar{Q} \quad (23)$$

$$gb \rightarrow b V_{\text{KK}} \rightarrow b Q\bar{Q} \quad (24)$$

where q stands for the light quarks present in the proton and Q/Q' stand for the final state heavy t and/or b quarks. Some generic Feynman diagrams are shown in Fig. 9. In the first case, a pair of b or t quarks is produced mainly in the gg fusion subprocess with a small contribution from $q\bar{q}$ annihilation, followed by the emission of a KK gauge boson from one of the heavy quark lines, while in the second case a KK gauge boson is emitted from the b -quark line in gb fusion with the initial b -quark taken from the proton sea. In both cases the produced KK gauge boson decays predominantly into heavy quark pairs, leading to topologies with multi b and/or t final states.

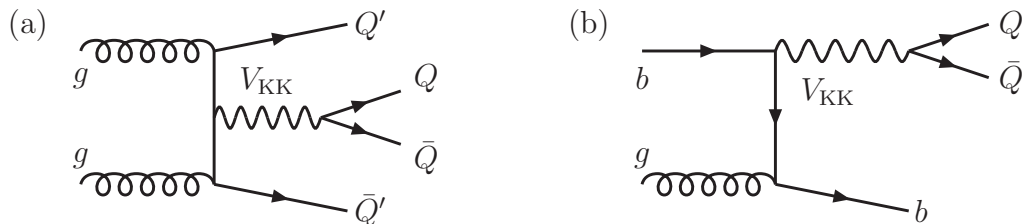


Figure 9: *Typical Feynman diagrams for associated V_{KK} production with $Q', Q = t, b$ quarks at the LHC: the four-body $gg \rightarrow QQ'Q'\bar{Q}$ (a) and the three-body $gb \rightarrow bQQ\bar{Q}$ (b) processes.*

In the $2 \rightarrow 4$ body reaction of eq. (23), since the SM production of quark pairs is dominated by the gg fusion mechanism, the largest contribution to associated production of KK gauge bosons with heavy quarks comes also from the same channel. After radiation from the heavy quark line, V_{KK} can either decay into a heavy quark pair of the same flavour as it was produced in association with, or of the other heavy flavour. To avoid the combinatorial background, we choose to look at $t\bar{t} + b\bar{b}$ final states which originate from the two channels $pp \rightarrow b\bar{b}V_{\text{KK}}$ with $V_{\text{KK}} \rightarrow t\bar{t}$ and $pp \rightarrow t\bar{t}V_{\text{KK}}$ with $V_{\text{KK}} \rightarrow b\bar{b}$. Since the $gg \rightarrow b\bar{b}$ cross section is much larger than the $pp \rightarrow t\bar{t}$ cross section and that the $t\bar{t}$ branching ratio of V_{KK} is in general larger than the $b\bar{b}$ branching ratio, the final $t\bar{t}b\bar{b}$ sample from the signal is dominantly originating from the subprocess $pp \rightarrow b\bar{b}V_{\text{KK}} \rightarrow b\bar{b}t\bar{t}$.

As for the kinematics of this production channel, the KK gauge boson is produced almost at rest owing to its large mass and hence decays into top quarks with a wide range of transverse momenta with an excess of events with large p_T . On the other hand, the b quarks produced in the hard process of gg fusion dominantly have small transverse momenta. The picture is reversed for the second channel $pp \rightarrow t\bar{t}V_{\text{KK}} \rightarrow t\bar{t}b\bar{b}$ which, as already mentioned, gives a smaller contribution to the signal cross section. For the QCD background that we have considered, $pp \rightarrow t\bar{t}b\bar{b}$, and that we have calculated using the code CompHEP [42], the dominant contribution comes from the subprocesses $gg/q\bar{q} \rightarrow t\bar{t}$ production followed by the emission of a virtual gluon splitting into a $b\bar{b}$ pair. To reduce this QCD background without significantly affecting the signal, we impose the following set of kinematical cuts

$$p_T^{t,\bar{t}} \geq 300 \text{ GeV}, \quad p_T^{b,\bar{b}} \geq 100 \text{ GeV}, \quad |\eta_{Q,\bar{Q}}| \leq 2. \quad (25)$$

We have used large cuts on the top quarks transverse momenta to reduce the background as much as possible; one can further optimize these cuts to improve the significance of the signal, but as the number of events will turn out to be rather small, we do not perform that analysis here. Additionally, we impose an opening angle cut $\theta_{b\bar{b}} \geq 60^\circ$ which reduces the gluon splitting into $b\bar{b}$ in the background by more than an order of magnitude and does not affect the signal much.

The cross-sections for $t\bar{t}b\bar{b}$ production are shown in Table 6 in all four RS scenarios E_1 to E_4 . The numbers for the RS model correspond to the signal only and do not include the background events or the interference with the background amplitudes [which should occur in the case where the KK excitation of the gluon is produced]. The rather low cross sections for signal events, compared to a SM background of $\sigma^{\text{SM}} \sim 0.4 \text{ fb}$, indicate that even with a high luminosity of $\mathcal{L} = 100 \text{ fb}^{-1}$, one will not be able to reach a significance of 5σ . The best significance, $\sim 4\sigma$, is obtained in the case of scenario E_2 . Hence, no discovery is possible with the $t\bar{t}b\bar{b}$ channel of associated production, if a reasonable luminosity is assumed. We expect the trend for the other topologies to be similar. Note that here, we considered only the production of the KK excitation of the gluon; the significance for the production of the KK excitations of the electroweak gauge bosons [and in particular of the $Z'^{(1)}$ which cannot be produced in the Drell–Yan processes discussed in section 3] is even smaller.

Next we turn to the associated production of the KK excitations with a b -quark in gb fusion. Though the density of b/\bar{b} quarks in the proton is small, the large coupling of the b -quark with the KK gluon for instance could partially compensate for it. Looking at the reaction $gb \rightarrow bg^{(1)} \rightarrow bt\bar{t}$, where b stands for both the b and the anti- b quark, we use the same kinematical cuts as those introduced in eq. (25). In fact, because now we are dealing with a $2 \rightarrow 3$ production process, the signal cross sections are expected to be one order of magnitude larger than that of the $2 \rightarrow 4$ process discussed previously. Here again, the b quark produced in the hard process has low transverse momentum, while the top quarks can have

	$\sigma^{\text{RS}}(pp \rightarrow t\bar{t}b\bar{b})$	$\sigma^{\text{RS}}/\sigma^{\text{SM}}$	$\mathcal{S}_{100}^{\text{ttbb}}$
E_1	0.06	0.13	0.8
E_2	0.26	0.58	3.9
E_3	0.04	0.08	0.6
E_4	0.16	0.35	2.3

Table 6: The signal cross section [fb], the signal to background ratio and the signal statistical significance for $\mathcal{L} = 100 \text{ fb}^{-1}$ for the four-body process $pp \rightarrow t\bar{t}b\bar{b}$ in the RS scenarios $E_{1,2,3,4}$ after the cuts discussed in the text are applied.

large transverse momenta in the signal events. The irreducible QCD background $bg \rightarrow b\bar{t}\bar{t}$, that we calculate again using CompHEP [42], is also more than one order of magnitude larger compared to the previous process, $\sigma^{\text{SM}} \sim 9 \text{ fb}$.

The signal production cross sections for a top quark pair and a b -type jet with the kinematical cuts of eq. (25) is shown in of Table 7 for the pure RS signal in the four selected scenarios $E_{1,\dots,4}$. Again the points E_2 and E_4 have large signal cross sections owing to the large coupling of the b quarks to the KK gluon. For the other two points, the couplings of b quark are small and, hence, lower production rates of the KK gluon are obtained. With an integrated luminosity of $\mathcal{L} = 100 \text{ fb}^{-1}$, one obtains a significance which is larger than 8 for scenarios E_2 and E_4 , while it is about 3 or less for the other two scenarios. We again have considered only the associated production of a KK gluon and not accounted for the interference between the RS signal and the background.

	$\sigma^{\text{RS}}(pp \rightarrow t\bar{t}b/t\bar{t}\bar{b})$	$\sigma^{\text{RS}}/\sigma^{\text{SM}}$	$\mathcal{S}_{100}^{\text{ttb}}$
E_1	0.91	0.10	3.0
E_2	4.12	0.47	13.8
E_3	0.61	0.07	2.0
E_4	2.50	0.28	8.4

Table 7: The signal cross section [fb], the signal to background ratio and the signal statistical significance for $\mathcal{L} = 100 \text{ fb}^{-1}$ for the three-body process $gb \rightarrow t\bar{t}b/t\bar{t}\bar{b}$ in the four RS scenarios $E_{1,2,3,4}$ after the cuts discussed in the text are applied.

Thus, at least in the 3-body production process $gb \rightarrow b\bar{t}\bar{t}$, the cross section in some RS scenarios can be significantly larger than the QCD background cross section. However, to reach a signal significance which is important, large integrated luminosities, $\mathcal{L} \gtrsim 100 \text{ fb}^{-1}$, are needed. In this case, the top and bottom quark jets cannot be identified with an excellent efficiency and more background processes with potentially much larger rates need

to be considered. Detailed experimental analyzes need thus to be performed in order to assess the viability of this signal.

5. Conclusions

In the framework of the Randall–Sundrum extra–dimensional model with SM fields in the bulk, we have studied the production of the KK excitations of gauge bosons at LHC which then dominantly decay into heavy top and bottom quark pairs. For illustration, we have considered a specific version of the model in which the SM gauge group is enhanced to a left–right symmetry and concentrated on quark geometrical localizations and gauge quantum numbers that allow to solve the LEP anomaly on the forward–backward asymmetry A_{FB}^b . We have selected some characteristic points of the parameter space of this model and assumed masses $M_{\text{KK}} \sim 3$ TeV for the KK excitations of the gluon and the electroweak gauge bosons as dictated by constraints from high–precision electroweak data.

We have shown that the contribution of the Drell–Yan process $q\bar{q} \rightarrow V_{\text{KK}} \rightarrow t\bar{t}$ to the $pp \rightarrow q\bar{q}/gg \rightarrow t\bar{t}$ cross section, in which we have taken into account the total width of the excitation as well as the interference between the signal and SM the background, can be substantial and would allow for the detection of the gluon KK excitation with a high statistical significance; the signal significance is smaller for the excitations of the electroweak gauge bosons as a result of the smaller couplings. Besides the invariant mass distributions and the sizeable total widths of the KK resonances, the polarization of the top quark and the forward–backward asymmetry, would allow to characterize the signal and to probe the chiral structure of the fermion couplings of the KK excitations. In the case of the $q\bar{q} \rightarrow V_{\text{KK}} \rightarrow b\bar{b}$ process, a large signal significance compared to the SM background is also obtained.

We have also calculated the cross sections for the higher order processes in which the KK excitations couple only to the heavy top and bottom quarks and compared them to their corresponding irreducible SM backgrounds. We have first studied the gluon–gluon fusion mechanism, $gg \rightarrow V_{\text{KK}} \rightarrow t\bar{t}, b\bar{b}$, which is induced by a heavy quark loop and in which the anomalous ggV_{KK} vertex has to be regulated via the Stückelberg mixing term. We have then analyzed the four–body reactions $pp \rightarrow t\bar{t}b\bar{b}, t\bar{t}t\bar{t}$ and $b\bar{b}b\bar{b}$ as well as the three–body reactions $gb \rightarrow bt\bar{t}$ and $bb\bar{b}$, in which the KK excitations are radiated from the heavy quark lines. The cross sections for these higher order processes at the LHC, except potentially for the $bg \rightarrow g^{(1)}b$ process, turn out to be too small⁽¹⁾ compared to the SM background, to allow for a detection of heavy KK excitations with $M_{\text{KK}} \gtrsim 3$ TeV.

In our parton–level analysis, we took into account only the irreducible SM QCD background and did not attempt to include experimental effects such as detection efficiencies, b –quark tagging, reducible light jet backgrounds etc.. Only refined and realistic Monte–Carlo analyses, which take into account all these effects, would allow to assess the viability of the

KK gauge boson signals. These experimental analyses are currently being performed by some members of the ATLAS and CMS collaborations [43]

Acknowledgments

We thank Fawzi Boudjema and Emilian Dudas for useful discussions on the anomaly cancellation in the $gg \rightarrow V_{\text{KK}}$ process, as well as Rohini Godbole and François Richard for useful suggestions. This work is supported by the CEFIPRA project no.3004-B and by the French ANR project PHYS@COL&COS.

References

- [1] L. Randall and R. Sundrum, Phys. Rev. Lett. 83 (1999) 3370; M. Gogberashvili, Int. J. Mod. Phys. D11 (2002) 1635.
- [2] A. Pomarol, Phys. Rev. Lett. 85 (2000) 4004; L. Randall and M.D. Schwartz, JHEP 0111 (2001) 003; Phys. Rev. Lett. 88 (2002) 081801; W.D. Goldberger and I.Z. Rothstein, Phys. Rev. D68 (2003) 125011; K. Choi and I.W. Kim, Phys. Rev. D67 (2003) 045005; K. Agashe, A. Delgado and R. Sundrum, Annals Phys. 304 (2003) 145.
- [3] K. Agashe and G. Servant, Phys. Rev. Lett. 93 (2004) 231805; JCAP 0502 (2005) 002; G. Bélanger, A. Pukhov and G. Servant, [arXiv: hep-ph/0706.0526](#).
- [4] T. Gherghetta and A. Pomarol, Nucl. Phys. B586 (2000) 141.
- [5] S. J. Huber and Q. Shafi, Phys. Lett. B498 (2001) 256; Phys. Lett. B544 (2002) 295; Phys. Lett. B583 (2004) 293; Phys. Lett. B512 (2001) 365; S. Chang *et al.*, Phys. Rev. D73 (2006) 033002; G. Moreau and J. I. Silva-Marcos, JHEP 0601 (2006) 048.
- [6] Y. Grossman and M. Neubert, Phys. Lett. B474 (2000) 361; T. Appelquist *et al.*, Phys. Rev. D65 (2002) 105019; T. Gherghetta, Phys. Rev. Lett. 92 (2004) 161601; G. Moreau, Eur. Phys. J. C40 (2005) 539.
- [7] M. Guchait, F. Mahmoudi and K. Sridhar, [arXiv: hep-ph/0703060](#).
- [8] G. Burdman, Phys. Rev. D66 (2002) 076003; C.S. Kim *et al.*, Phys. Rev. D67 (2003) 015001; J.L. Hewett, F.J. Petriello and T.G. Rizzo, JHEP 0209 (2002) 030; S.J. Huber and Q. Shafi, Phys. Rev. D63 (2001) 045010; S.J. Huber, C.A. Lee and Q. Shafi, Phys. Lett. B531 (2002) 112; C. Csaki *et al.*, Phys. Rev. D66 (2002) 064021.
- [9] K. Agashe, A. Delgado, M. J. May and R. Sundrum, JHEP 0308 (2003) 050.

- [10] M. Carena, E. Pontón, T. Tait and C. Wagner, Phys. Rev. D67 (2003) 096006; M. Carena *et al.*, Phys. Rev. D68 (2003) 035010; Phys. Rev. D71 (2005) 015010; F. del Aguila, M. Perez-Victoria and J. Santiago, JHEP 0302 (2003) 051; M. Carena, T. Tait and C. Wagner, Acta Phys. Polon. B33 (2002) 2355.
- [11] A. Delgado and A. Falkowski, arXiv: hep-ph/0702234.
- [12] K. Agashe, R. Contino, L. Da Rold and A. Pomarol, Phys. Lett. B641 (2006) 62.
- [13] A. Djouadi, G. Moreau and F. Richard, Nucl. Phys. B773 (2007) 43.
- [14] The LEP Collaborations (ALEPH, DELPHI, L3 and OPAL), the LEP Electroweak Working Group and the SLD Heavy Flavour Group, *A combination of preliminary Electroweak measurements and constraints on the Standard Model*, Phys. Rep. 427 (2006) 257, arXiv: hep-ex/0509008, <http://lepewwg.web.cern.ch/LEPEWWG>.
- [15] For a review, see: K. Monig, Rept. Prog. Phys. 61 (1998) 999.
- [16] A. Djouadi, J. Kühn and P. M. Zerwas, Z. Phys. C46 (1990) 411.
- [17] G. Cacciapaglia, C. Csáki, G. Marandella and J. Terning, Phys. Rev. D75 (2007) 015003; M. Carena, E. Pontón, J. Santiago and C. Wagner, Nucl. Phys. B759 (2006) 202; M. Carena, E. Pontón, J. Santiago and C. Wagner, arXiv: hep-ph/0701055.
- [18] S. J. Huber, Nucl. Phys. B666 (2003) 269; G. Moreau and J. I. Silva-Marcos, JHEP 0603 (2006) 090.
- [19] K. Agashe *et al.*, Phys. Rev. Lett. 93 (2004) 201804; Phys. Rev. D71 (2005) 016002.
- [20] Z. Ligeti, M. Papucci and G. Perez, Phys. Rev. Lett. 97 (2006) 101801; K. Agashe *et al.*, arXiv: hep-ph/0509117; K. Agashe *et al.*, Phys. Rev. D74 (2006) 053011; Phys. Rev. D75 (2007) 015002.
- [21] F. Ledroit, G. Moreau and J. Morel, arXiv: hep-ph/0703262.
- [22] E. De Pree and M. Sher, Phys. Rev. D73 (2006) 095006.
- [23] K. Agashe *et al.*, arXiv: hep-ph/0701186; A. Liam Fitzpatrick *et al.*, arXiv: hep-ph/0701150.
- [24] C. Dennis *et al.*, arXiv: hep-ph/0701158.
- [25] For GUTs Z' physics at hadron colliders, see for instance: J.L. Hewett and T.G. Rizzo, Phys. Rept. 183 (1989) 193; A. Leike, Phys. Rept. 317 (1999) 143. For a more recent analysis, see: M. Dittmar *et al.*, Phys. Lett. B583 (2004) 111.

- [26] H. Davoudiasl, J. Hewett and T. Rizzo, Phys. Rev. D63 (2001) 075004.
- [27] B. Lillie, L. Randall and L.-T. Wang, arXiv: hep-ph/0701166.
- [28] K. Agashe *et al.*, arXiv: hep-ph/0612015.
- [29] D. Choudhury, R. M. Godbole, R. K. Singh and K. Wagh, arXiv:0705.1499 [hep-ph].
- [30] C. A. Scrucca and M. Serone, Int. J. Mod. Phys. A19 (2004) 2579.
- [31] T. Han, G. Valencia and Y. Wang, Phys. Rev. D70 (2004) 034002 and Int. J. Mod. Phys. A20 (2005) 3214.
- [32] K. Agashe, R. Contino and A. Pomarol, Nucl. Phys. B719 (2005) 165.
- [33] A. Delgado, A. Pomarol and M. Quiros, JHEP 0001 (2000) 030.
- [34] J. Pumplin, D. Stump, J. Huston, H. L. Lai, P. Nadolsky and W. K. Tung, (CTEQ Collaboration), JHEP 0207 (2002) 012.
- [35] R.M. Godbole, S.D. Rindani and R.K. Singh, JHEP 0612 (2006) 021.
- [36] P. Binétruy, C. Deffayet, E. Dudas and P. Ramond, Phys. Lett. B441 (1998) 163.
- [37] N. Arkani-Hamed, A. G. Cohen and H. Georgi, Phys. Lett. B516 (2001) 395.
- [38] T. Hirayama and K. Yoshioka, JHEP 0401 (2004) 032.
- [39] C. T. Hill, Phys. Rev. D73 (2006) 085001.
- [40] C. A. Scrucca, M. Serone, L. Silvestrini and F. Zwirner, Phys. Lett. B525 (2002) 169.
- [41] P. Anastasopoulos, M. Bianchi, E. Dudas and E. Kiritsis, JHEP 0611 (2006) 057.
- [42] A. Pukhov *et al.*, CompHEP, arXiv: hep-ph/9908288.
- [43] G. Brooijmans et al. [for the ATLAS Collaboration] and C.H. Shepherd-Themistocleous et al. [for the CMS Collaboration], work in progress. We thank these authors for discussions about these processes during the Les Houches Workshop.